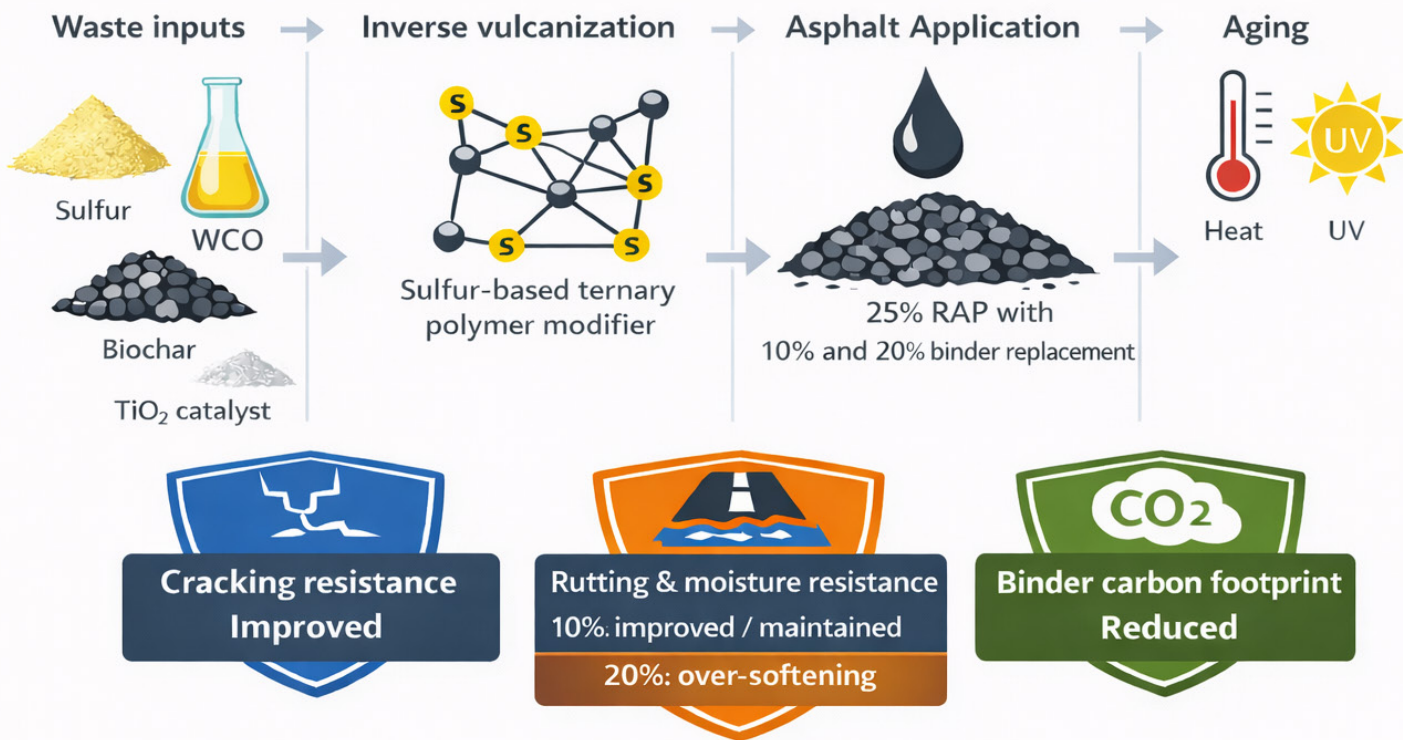


# Enhancing Sustainability and Durability in Asphalt Pavements: Evaluating the Impact of Low-Carbon Sulfur Polymer Modifiers and Reclaimed Asphalt Pavement

Mohammad Doroudgar, MS

Shadi Saadeh, PhD

Elham Fini, PhD



# MINETA TRANSPORTATION INSTITUTE

Founded in 1991, the Mineta Transportation Institute (MTI), an organized research and training unit in partnership with the Lucas College and Graduate School of Business at San José State University (SJSU), increases mobility for all by improving the safety, efficiency, accessibility, and convenience of our nation's transportation system. Through research, education, workforce development, and technology transfer, we help create a connected world. MTI leads the [California State University Transportation Consortium \(CSUTC\)](#) funded by the State of California through Senate Bill 1 and the Rail Resilience to Severe Weather: Training and Research Program (RR2SW) funded by the Federal Railroad Administration. MTI focuses on three primary responsibilities:

## Research

MTI conducts multi-disciplinary research focused on surface transportation that contributes to effective decision making. Research areas include: active transportation; planning and policy; security and counterterrorism; sustainable transportation and land use; transit and passenger rail; transportation engineering; transportation finance; transportation technology; and workforce and labor. MTI research publications undergo expert peer review to ensure the quality of the research.

## Education and Workforce Development

To ensure the efficient movement of people and goods, we must prepare the next generation of skilled transportation professionals who can lead a thriving, forward-thinking transportation industry for a more connected world. To help achieve this, MTI sponsors a suite of workforce development and education opportunities. The Institute supports educational programs offered by the Lucas Graduate School of Business: a Master of Science in Transportation Management, plus graduate certificates that include High-Speed and Intercity Rail Management and Transportation Security Management. These flexible programs offer live online classes so that working transportation professionals can pursue an advanced degree regardless of their location.

## Information and Technology Transfer

MTI utilizes a diverse array of dissemination methods and media to ensure research results reach those responsible for managing change. These methods include publication, seminars, workshops, websites, social media, webinars, and other technology transfer mechanisms. Additionally, MTI promotes the availability of completed research to professional organizations and works to integrate the research findings into the graduate education program. MTI's extensive collection of transportation-related publications is integrated into San José State University's world-class Martin Luther King, Jr. Library.

---

## Disclaimer

The contents of this report reflect the views of the authors, who are responsible for the facts and accuracy of the information presented herein. This document is disseminated in the interest of information exchange. MTI's research is funded, partially or entirely, by grants from the U.S. Department of Transportation, the California Department of Transportation, and the California State University Office of the Chancellor, whom assume no liability for the contents or use thereof. This report does not constitute a standard specification, design standard, or regulation.

Report 26-09

# **Enhancing Sustainability and Durability in Asphalt Pavements: Evaluating the Impact of Low-Carbon Sulfur Polymer Modifiers and Reclaimed Asphalt Pavement**

Mohammad Doroudgar, MS  
Shadi Saadeh, PhD  
Elham Fini, PhD

June 2026

A publication of the  
**Mineta Transportation Institute**  
Created by Congress in 1991

College of Business  
San José State University  
San José, CA 95192-0219

# Technical Report Documentation Page

<b>1. Report No.</b> 26-09	<b>2. Government Accession No.</b>	<b>3. Recipient's Catalog No.</b>	
<b>4. Title and Subtitle</b> Enhancing Sustainability and Durability in Asphalt Pavements: Evaluating the Impact of Low-Carbon Sulfur Polymer Modifiers and Reclaimed Asphalt Pavement		<b>5. Report Date</b> June 2026	
		<b>6. Performing Organization Code</b>	
<b>7. Authors</b> Mohammad Doroudgar, MS Shadi Saadeh, PhD Elham Fini, PhD		<b>8. Performing Organization Report</b> CA-MTI-2522	
<b>9. Performing Organization Name and Address</b> Mineta Transportation Institute College of Business San José State University San José, CA 95192-0219		<b>10. Work Unit No.</b>	
		<b>11. Contract or Grant No.</b> SB1-SJAUX_2023-26	
<b>12. Sponsoring Agency Name and Address</b> State of California SB1 2017/2018 Trustees of the California State University Sponsored Programs Administration 401 Golden Shore, 5th Floor Long Beach, CA 90802		<b>13. Type of Report and Period Covered</b>	
		<b>14. Sponsoring Agency Code</b>	
<b>15. Supplemental Notes</b> 10.31979/mti.2026.2522			
<b>16. Abstract</b> <p>The asphalt industry faces major challenges, including the need for pavements that last longer and are more sustainable, as traditional asphalt production is costly and has a high environmental impact. To address this, researchers have been exploring modified asphalt binders such as rubber, charcoal, and waste cooking oil, which have shown promise in extending the lifespan, resistance to deformation, and durability of asphalt pavements. In addition, governments and industries are investing in the use of recycled and “green” materials to reduce the carbon footprint and environmental degradation of conventional asphalt mixtures. Building on this momentum, this study investigates the performance of a low-carbon modifier consisting of a composite of sulfur, biochar, and waste cooking oil in the conventional hot mix asphalt mixture with 25% reclaimed asphalt pavement (RAP). The modifier was introduced at 10% and 20% by the total weight of the asphalt binder, representing an asphalt mixture with 11.5% and 22.4% reduction in carbon footprint compared to typical asphalt binder, following Park et al. (2024). To understand how these lower-carbon mixtures perform in the real world, researchers used two standard tests: the Indirect Tensile Asphalt Cracking Test (IDEAL-CT) and Hamburg Wheel Tracking Test (HWT), which examined the fracture (cracking) and rutting resistance of the resulting mixtures, respectively. Extended thermal aging and UV aging were applied to study the effect of long-term aging on each scenario. Two types of aging are used, long-term aging following NCHRP (Report 973) and UV aging following Rajib and Fini (2020). The study results showed that introducing the low-carbon modifier led to less reduction in resistance to aging as measured by fracture resistance and rutting durability compared to the control scenario. This means that they maintained stronger resistance to cracking and rutting even after aging while also reducing the carbon footprint of the mixture by up to 22.4%. This research demonstrates that meaningful reductions in the carbon footprint of asphalt pavements can be achieved without compromising long-term structural performance or durability, supporting more sustainable and resilient transportation infrastructure.</p>			
<b>17. Key Words</b> Polymer asphalt, hot mix asphalt (HMA), reclaimed asphalt pavement (RAP), asphalt additives, asphalt mixtures		<b>18. Distribution Statement</b> No restrictions. This document is available to the public through The National Technical Information Service, Springfield, VA 22161.	
<b>19. Security Classif. (of this report)</b> Unclassified	<b>20. Security Classif. (of this page)</b> Unclassified	<b>21. No. of Pages</b> 76	<b>22. Price</b>

Copyright © 2026  
by **Mineta Transportation Institute**  
All rights reserved.

DOI: 10.31979/mti.2026.2522

Mineta Transportation Institute  
College of Business  
San José State University  
San José, CA 95192-0219

Email: [mineta-institute@sjsu.edu](mailto:mineta-institute@sjsu.edu)

[transweb.sjsu.edu/research/2522](https://transweb.sjsu.edu/research/2522)

## **Acknowledgments**

I would like to begin by expressing my sincere gratitude to Dr. Elham Fini for her exceptional guidance and expertise in binder modification, which greatly enriched this research. I am deeply thankful to Dr. Shadi Saadeh for his unwavering support, mentorship, and patience throughout this journey. This work would not have been possible without him. Special thanks go to Vulcan Materials Company for generously providing the binder and aggregates used in this study. I am also grateful to G3 Quality, California, for their valuable assistance in fabricating the Hamburg Wheel Track Test samples. A heartfelt acknowledgment goes to Roger Khoudessian, Kreetha Mekchai, Mohammadjavad Kazemi, and Gregory Reader for their insightful guidance and contributions to the development of this project. Lastly, I am profoundly thankful to my parents for their constant encouragement and support, without which achieving my goals would not have been possible. The author thanks Lisa Rose and Editing Press for editorial services, as well as MTI staff Project Assistant, Rajeshwari Rajesh, and Graphic Design Assistant, Katerina Earnest.

# Contents

<b>Acknowledgments</b>	<b>vi</b>
<b>List of Figures</b>	<b>ix</b>
<b>List of Tables</b>	<b>x</b>
<b>Executive Summary</b>	<b>1</b>
<b>1. Introduction</b>	<b>2</b>
<b>2. Literature Review</b>	<b>5</b>
2.1 Low-Carbon and Sustainable Asphalt Modifiers	5
2.2 Application of Reclaimed Asphalt Pavement (RAP) and Rejuvenators	7
2.3 Synergistic or Hybrid Binder Modification Strategies	8
2.4 Aging Behavior and Long-Term Performance of Asphalt Mixtures	11
2.5 Testing Protocols and Performance Evaluation	13
<b>3. Objective</b>	<b>15</b>
<b>4. Materials</b>	<b>17</b>
4.1 Aggregate	17
4.2 Asphalt Binder	17
4.3 Reclaimed Asphalt Pavement (RAP)	17
4.4 Additives	18
<b>5. Methodology</b>	<b>20</b>
5.1 Mixing and Sample Preparation	20
5.2 Aging	22
5.3 Compaction and Fabrication	24
<b>6. Testing Method</b>	<b>28</b>
6.1 Indirect Tensile Asphalt Cracking Test	28
6.2 Hamburg Wheel Tracking Test	31
<b>7. Results and Analysis</b>	<b>33</b>
7.1 Hamburg Wheel Tracking Test	33
7.2 Indirect Tensile Asphalt Cracking Test	41
<b>8. Summary and Conclusions</b>	<b>56</b>
8.1 Conclusions	56
8.2 Limitations and Recommendations	57

<b>Bibliography</b>	<b>59</b>
<b>About the Authors</b>	<b>64</b>

## List of Figures

Figure 1. Aggregate Gradation Curve	17
Figure 2. Shear Mixer Used for This Project	20
Figure 3. Control Mix After Short-Term Aging	21
Figure 4. Mobile Mixer to Mix Aggregates with Binder	22
Figure 5. UV Chamber	24
Figure 6. Vacuum Saturation of Conditioned Loose Asphalt Mixture and Shaker	25
Figure 7. Superpave Gyratory Compactor for Specimen Compaction	27
Figure 8. DTS Machine for IDEAL-CT Testing	31
Figure 9. Hamburg Wheel Track Test Setup After Test	32
Figure 10. Average Rut Depth at 15,000 Passes	35
Figure 11. Rut Depth vs No. of Passes for Mixtures Without Aging	36
Figure 12. Rut Depth vs No. of Passes for Mixtures at 3 Days of Aging	36
Figure 13. Rut Depth vs No. of Passes for Mixtures at 5 Days of Aging	37
Figure 14. Rut Depth vs No. of Passes for Mixtures at 7 Days of Aging	37
Figure 15. Rut Depth vs No. of Passes for Mixtures at Thermally + UV Aging Level	37
Figure 16. CTindex for Mixtures	46
Figure 17. Load vs Deformation Curves for Mixtures at Without Aging Level	48
Figure 18. Load vs Deformation Curves for Mixtures at 3 Days of Aging Level	48
Figure 19. Load vs Deformation Curves for Mixtures at 5 Days of Aging Level	49
Figure 20. Load vs Deformation Curves for Mixtures at 7 Days of Aging Level	49
Figure 21. Load vs Deformation Curves for Mixtures at Thermally + UV Aging Level	50
Figure 22. Peak Load vs Level of Aging	51

## List of Tables

Table 1. Test Factorial	16
Table 2. Asphalt Binder Properties	19
Table 3. Hamburg Wheel Rut Depth Results at 15,000 Passes	34
Table 4. ANOVA Results Rut Depth at 15,000 passes	38
Table 5. One-Way ANOVA of 15000 Pass Rut Depths by Aging Level	39
Table 6. Tukey Pair-Wise Comparison Table for Rut Depth at 15,000 Passes	40
Table 7. IDEAL-CT Results for Each Mixture at Without Aging Level	42
Table 8. IDEAL-CT Results for Each Mixture at 3 Days of Aging Level	43
Table 9. IDEAL-CT Results for Each Mixture at 5 Days of Aging Level	44
Table 10. IDEAL-CT Results for Each Mixture at 7 Days of Aging Level	45
Table 11. IDEAL-CT Results for Each Mixture at Thermally + UV Aging Level	46
Table 12. T-Test for Pair wise CTindex Comparisons at Each Aging Level	52
Table 13. Tukey HSD Pair-Wise Comparisons of CTindex Aging Level	54
Table 14. Summary of Test Results by Level of Aging	54
Table 15. Summary of Tukey Pair wise Comparison for All Tests	55

## Executive Summary

Public infrastructure officials share a desire to implement sustainable practices and greener policies. Today, sustainable practices have not only become more common but are also associated with ending the use of virgin asphalt which has a negative effect on the environment. The extensive use of asphalt pavements may consume more virgin materials, and they are also more vulnerable to criticisms concerning rutting, cracking, and aging. Despite the existence of Reclaimed Asphalt Pavement (RAP) in the industry, it is underused and may be a downgrade if it is not co-used with proper modifiers.

In this research, an investigation took place into a sulfur polymer system that aimed to lower greenhouse gases. Sulfur, waste cooking oil, and biochar waste were blended into an asphalt mixture with an addition of 25% RAP. This was done in parallel with a test considering the standard addition of blends. The aim is to tackle problems related to cracking and the deformation of pavements and to evaluate the attained lower waste pavements and make the pavement last longer.

The testing in the laboratory was done under standard conditions. To simulate the service life in a laboratory, the mixtures were subjected to thermal aging for 3, 5, and 7 days, in addition to a separate test under ultraviolet light to simulate long-term weathering. The Hamburg Wheel Tracking Test (HWT) was applied at 50°C in order to assess rutting performance with up to 20,000 applied cycles as well as the IDEAL Cracking Test (IDEAL-CT) in order to assess cracking resistance. The data regarding stiffness and rut depth were collected for deeper analysis in accordance with the aging level.

The test shows clear improvements after the polymer inclusion. The mix balance shows better cracking of the 10% blend under UV exposure. The rutting criteria of the “no aging” untimely condition shows failure in the 20% blend, while after aging showed the mix offered decent rutting. Both of the modified blends did better in one of the defined criteria in comparison to the control, and the 10% blend is better in terms of balancing the properties.

# 1. Introduction

Asphalt mixtures play a significant role in the development of infrastructure worldwide, paving vast roadway networks necessary for transportation and economic development. The asphalt pavement industry faces huge challenges concerning sustainability and durability. Conventional hot mix asphalt (HMA) is the most common pavement mixture; it is prone to distresses such as rutting, cracking, and aging by oxidation. This reduces the pavement's lifespan, leading to more frequent maintenance and economic burdens (Bilema et al., 2021).

The conventional production of asphalt mixtures exerts a considerable environmental impact due to its energy-intensive processes. The production and application of asphalt mixtures emit significant quantities of carbon dioxide (CO<sub>2</sub>), thereby challenging the pavement industry's role in global greenhouse gas emissions (Majidifard et al., 2019). This environmental challenge resonates with global efforts to reach carbon neutrality and underscores the pressing need for the adoption of sustainable, low-carbon materials and technologies in asphalt paving (Luo & Zhang, 2023).

Additionally, environmental exposure and aging factors accelerate pavement deterioration. Asphalt binders rapidly age through oxidative mechanisms driven by ultraviolet (UV) radiation and elevated temperatures. The aged binder loses much of its flexibility while developing significant stiffness and brittleness, which causes the pavement surface to exhibit numerous cracks and premature failures. Therefore, aging goes against the basic principle of sustainable infrastructure and calls for innovative methods to prevent such aging from ever occurring and causing deterioration and environmental hazards (Mousavi et al., 2023).

The U.S. Federal Highway Administration (FHWA) has initiated several projects aimed at significantly reducing greenhouse gas emissions in highway construction, recognizing the importance of these environmental and performance-related issues. In 2022, the Federal Highway Administration (FHWA) established the Climate Challenge Initiative and provided \$7.1 million to 25 state departments of transportation to help pay for projects and technologies that lower carbon footprints and make pavement infrastructures more sustainable (Federal Highway Administration [FHWA], 2022). The U.S. General Services Administration (GSA) mandated that construction contractors give Environmental Product Declarations (EPDs) for asphalt materials and pushed for more environmentally friendly methods, such as using more recycled asphalt pavement (RAP), warm-mix asphalt technology, and bio-based or alternative asphalt binders (U.S. General Services Administration [GSA], 2022). These efforts make it obvious that developing sustainable pavement technologies is a national priority and a matter of great urgency. They also give a solid reason to investigate new asphalt mixtures that use eco-friendly additives.

These policy-driven actions underscore the urgency and national priority of advancing sustainable pavement technologies and provide a strong rationale for exploring innovative asphalt mixtures incorporating environmentally friendly additives. Recent research has focused on adding waste-derived and bio-based materials such as reclaimed asphalt pavement (RAP), waste cooking oil (WCO), and biochar to asphalt mixtures to make them last longer. RAP greatly cuts down on the need for new aggregates and binders, which lowers production costs and impacts on the environment. However, if not properly rejuvenated, its high stiffness can make it less flexible and cause it to crack at an early stage. Waste cooking oil can be an affordable additive to bring back the ductility of old binders. Dugan et al. (2020) showed that mixing WCO with binders that have a lot of RAP in them made them much better at flowing, which made the binder softer and improved its long-term performance. Simultaneously, biochar, a carbon-dense byproduct of biomass pyrolysis, has demonstrated significant promise in enhancing binder aging resistance. According to Rajib et al. (2021), biochar made from biomass that is high in lipids and proteins can protect bituminous materials from damage caused by UV light by getting rid of free radicals and making them more chemically stable. These eco-friendly additives not only make mixtures stronger and last longer, but they also encourage circular economic practices by turning waste streams into infrastructure uses.

The long-term performance of asphalt pavements is still heavily influenced by aging. Over time, heat, oxygen, and ultraviolet (UV) radiation cause the binder to oxidize, making it stiffer and less flexible. This eventually leads to cracks in the surface and early pavement failure. High service temperatures or adverse environmental conditions often accelerate long-term oxidative aging. UV exposure, on the other hand, causes photochemical degradation, especially in thin surface layers. Asphalts with high RAP contents are especially weak because their binders are already old. Previous research has demonstrated that traditional modifiers can partially retard aging; however, many inadequately safeguard the binder against UV-induced damage. Rajib et al. (2021) showed that biochar can absorb UV light and free radicals, which slows down aging caused by UV light by making the binder matrix more chemically stable. Adding these kinds of components may be the key to making asphalt mixtures last longer in the field.

The effects of sulfur, biochar, and waste cooking oil on asphalt binder properties have all been the subject of numerous studies; however, not much is available about how these modifiers work together in a reclaimed asphalt mixture at the mixture level. Using laboratory aging protocols such as the Rolling Thin Film Oven (RTFO) and Pressure Aging Vessel (PAV), previous work by Fini et al. and others has mostly concentrated on binder-level performance, which may not accurately reflect field aging at the mixture scale. Moreover, conventional laboratory studies rarely examine the effects of UV radiation, as a significant cause of surface pavement aging. The adoption of sustainable additives, which may behave differently in complex mixtures than in isolated binder systems, makes this gap particularly significant. By evaluating the long-term performance of hot

mix asphalt (HMA) containing RAP, sulfur, WCO, and biochar, this study aims to close this gap under both thermal and UV aging situations.

This research will concentrate on the evaluation of sustainable and durable hot mix asphalt (HMA) mixtures containing 25% reclaimed asphalt pavement (RAP) and modified with low-carbon sulfur, waste cooking oil (WCO), and biochar additives. The experimental design simulates multiple aging scenarios to reflect long-term field conditions using both thermal aging and ultraviolet (UV) exposure. Thermal aging was performed according to the NCHRP Report 973 protocol for 3, 5, and 7 days through oven aging at 95°C. A separate aging scenario combined 3-day thermal aging followed by UV exposure at 50–55°C for 72 hours using a fluorescent UV lamp at 315–400 nm, based on protocols validated by Rajib et al. (2021). The mechanical performance of each mixture was assessed through two key laboratory tests: the Indirect Tensile Asphalt Cracking Test (IDEAL-CT) to evaluate fracture resistance and the Hamburg Wheel Tracking Test (HWT) to measure rutting susceptibility. These procedures were selected to simulate the environmental and mechanical stresses that asphalt pavements undergo during their service life in Southern California.

## 2. Literature Review

### 2.1 Low-Carbon and Sustainable Asphalt Modifiers

The shift toward sustainable, low-carbon binder modifiers has been encouraged by the environmental impact of asphalt pavement construction. In particular, during high-temperature processing and during the pavement's service life, petroleum-based binders are energy-intensive to produce and significantly increase greenhouse gas emissions (Pahlavan et al., 2021; Saadeh et al., 2023). The aging susceptibility of conventional binders worsens this problem by stiffening and losing ductility as a result of oxidative and ultraviolet (UV) exposure, which causes cracking and early pavement failure (Rajib et al., 2021; Majidifard et al., 2019). In order to solve this challenge, a wide range of sustainable modifiers has been explored and tested. Among these, biochar, sulfur, waste cooking oil (WCO), and crumb rubber have shown promise in improving binder performance while reducing negative effects on the environment (Rajib & Fini, 2020; Luo & Zhang, 2023; Zhou et al., 2021).

Considering all of its applications, biochar, a carbon-rich residue made through biomass pyrolysis, has drawn a lot of interest. It can function as a UV shield and a free-radical scavenger due to its porous structure and antioxidant properties. By limiting oxygen diffusion and absorbing UV radiation, algal biochar was shown by Rajib and Fini (2020) to reduce UV-induced binder aging by up to 36%. The significance of surface functional groups, like carboxyl, in neutralizing oxidation reactions was also indicated by their findings. Another investigation by Rajib et al. (2021) demonstrated that adding biochar to rubberized asphalt enhanced aging resistance considerably by working in conjunction with carbon black, as evidenced by reduced aging indices and maintained surface morphology. In comparison to conventional and rubberized mixes, Saadeh et al. (2023) found that biochar-enhanced hot mix asphalt (HMA) performed better in terms of cracking and rutting in both the HWT and Semi-Circular Bending (SCB) tests. However, the pyrolysis conditions, dosage, and feedstock origin all affect how well biochar performs, so careful optimization is required for wider field use.

Furthermore, waste cooking oil (WCO) has been investigated as an environmentally friendly solution. It is a good rejuvenator because of its low viscosity and chemical compatibility with aged binders. In their investigation of WCO's rejuvenating effects, Luo and Zhang (2023) discovered that it not only reduced mixing and compaction temperatures but also successfully restored the stiff binders' ductility and flow characteristics. According to Dugan et al. (2020), adding 10% WCO to high-RAP binders decreased viscosity without sacrificing fatigue resistance or desirable Superpave grades. Moreover, their study indicates that when blends with 60% RAP were rejuvenated with WCO, they demonstrate promising results in terms of rutting and fatigue.

After Majidifard et al. (2019) assessed WCO in rubberized binders, they found increasing the amount of recycling agent in the high-RAP mixtures improved their workability and low temperature performance while decreasing moisture damage and rutting resistance. However, they and others pointed out that a high WCO content might oversoften the binder, jeopardizing its moisture stability and resistance to rutting. This emphasizes how crucial dosage control is, particularly in hybrid systems that use rubberized binders or RAP.

Crumb rubber, which is a recycled waste product of tires, increases the elasticity and fatigue resistance of binder. Over time, though, its high stiffness and oxidative sensitivity may prove harmful. Researchers have looked into rubber–WCO hybrid systems as a solution to these problems. Using atomic force microscopy (AFM) to evaluate rubber-oil binders at the nanoscale, Lyu et al. (2021) demonstrated that WCO improved surface stability by softening the stiff crystalline domains in the rubberized binder. In addition to more consistent domain structures and enhanced surface integrity under thermal aging, their results showed performance gains of 35–100% across a range of aging indices. Although these nanoscale results are encouraging, there is still a lack of full-scale mixture analyses, which suggests a need for more study.

Due to its cost-effectiveness and cross-linking properties, sulfur, an abundant industrial byproduct, is another additive of interest. By creating crystalline structures inside the binder, sulfur functions as a curing agent when added in low quantities, improving stiffness and elasticity. Sulfur-modified rubber-bio-oil binders were assessed by Zhou et al. (2021), who found improvements in elastic recovery, viscosity control, and softening point. The advantages were attributed to sulfur's ability to facilitate chemical reactions between the components of the binder and unsaturated oils. However, their study also pointed out that an excessive amount of sulfur could cause the binder to become brittle, indicating that the benefits of sulfur are best experienced in combination with antioxidants such as biochar or softer modifiers such as WCO. More research is still needed in the areas of dosage optimization and field-scale validation.

Emerging materials have also been investigated in addition to these fundamental modifiers. Carbonitride-based modifiers (CNDC), which are created by grafting organic compounds into inorganic carriers, were first presented by Jiang et al. (2021). These binders showed enhanced UV stability and resistance to rutting. Likewise, Technisoil G5, a binder containing recycled plastic, was investigated by Saadeh et al. (2021). Although it supported completely recycled mixtures and demonstrated sustainability benefits, its fracture energy and cracking resistance fell short of those of traditional PG-graded binders. Although these innovative additives have specialized uses, more research is needed to evaluate their long-term performance in field conditions, constructability, and cost.

Finally, research indicates that low-carbon modifiers have the potential to improve asphalt performance while meeting environmental goals. The most promising materials among those

under study are biochar, WCO, sulfur, and crumb rubber, and their combined potential is even greater in hybrid systems. There are still gaps in our knowledge of their interaction mechanisms, mixture-level effects, and aging behavior under real-world circumstances.

## **2.2 Application of Reclaimed Asphalt Pavement (RAP) and Rejuvenators**

Reclaimed Asphalt Pavement (RAP) in road construction has gained more attention in recent years due to environmental and cost benefits. RAP can significantly decrease construction costs, reduce dependency on virgin aggregates and binders, and cut greenhouse gas emissions. Aged RAP binders, on the other hand, have low ductility and high stiffness, which reduces fatigue resistance and raises the risk of pavement cracking early in its life. To restore aged binder properties without sacrificing structural integrity, these challenges present an opportunity for researchers to investigate rejuvenation techniques and performance-based mix designs (Sedthayutthaphong et al., 2021; Bilema et al., 2021).

The incomplete blending of aged and virgin binders is a significant issue in mixtures with high RAP content, as it frequently leads to inconsistent stiffness and unpredictable mixture behavior. In a study of the friction and skid resistance of hot mix asphalt containing RAP, Sedthayutthaphong et al. (2021) found that aging-related hardening decreased ductility and accelerated polishing under traffic. Similar to this, Kar et al. (2017) assessed foamed bituminous mixtures with different percentages of RAP and discovered that, although RAP improved stability and decreased deformation, it also decreased workability and flexibility, particularly at higher contents. These studies show that RAP binders need chemical rejuvenation to restore performance.

Vegetable oils and frying oils have become popular as affordable, eco-friendly rejuvenators since they soften and work well with old asphalt. Dugan et al. (2020) showed that mixes of virgin asphalt with up to 60% RAP binder and 10% waste vegetable oil (WVO) kept their rheological and fatigue properties. Their research shows that WVO makes flow and flexibility better by restoring the right balance of asphaltenes and maltenes in old binders. Bilema et al. (2021) enhanced penetration values, softening points, and elastic recovery by combining WVO with crumb rubber, showcasing effective stiffness and aging mitigation. These findings show the effect of the hybrid rejuvenation system in overcome the limitation of RAP.

Luo and Zhang (2023) additionally explored a number of different ways to rejuvenate materials and found that WVO was effective at restoring ductility and lowering compaction temperatures. In addition, different approaches for rejuvenation were explored by Luo and Zhang (2023), which showed that WVO was effective at restoring ductility and lowering compaction temperatures. However, Luo and Zhang warned that too much WVO could make mixtures too soft, which would make them less resistant to rutting and moisture in compare to typical mixtures. This sensitivity

to dosage was also seen in the work of Zhang et al. (2022), who looked at rejuvenated fiber-reinforced mixtures in conditions that made them more likely to absorb moisture. Their findings indicated that moderate utilization of WVO alongside reinforcing fibers provided a significant cost-performance benefit, especially in challenging environmental conditions.

Other approaches, such as emulsified asphalt recycling and cold in-place recycling, have also been looked into as ways to effectively use high RAP contents. Unger Filho et al. (2020) showed that a cold-recycled base course made up entirely of RAP and emulsified asphalt was strong enough for use as a subbase. Their work shows how changing the way things are done, including lowering mixing temperatures or using emulsion-based binders, can make full-depth RAP use more sustainable and easier to build.

The environmental advantages of RAP and rejuvenators surpass material reutilization alone. Wei et al. (2021) examined volatile organic compound (VOC) emissions during mixing and determined that WVO contributed to the reduction of emissions in RAP mixtures. A life-cycle analysis conducted by Siverio Lima et al. (2020) supported the sustainability advantages of RAP, indicating significant energy savings and emissions reductions when implemented on urban roads in Münster, Germany. These results show that RAP is in line with environmental goals, but performance trade-offs are still major concerns.

Coleri et al. (2021) performed mechanistic–empirical simulations and life-cycle cost analyses to evaluate high-RAP mixtures from a performance-cost standpoint. Their findings indicated that with suitable rejuvenator dosing, mixtures containing up to 40% RAP attained long-term performance akin to conventional mixes, while providing substantially reduced maintenance expenses. These studies together show that performance-based high-RAP designs are possible, but they also show that we don't fully understand how RAP, rejuvenators, and modifiers work together when they age in the field.

Although many of these studies have demonstrated favorable outcomes, there are still gaps in the consistency of blending, dosage optimization, and long-term aging behavior of rejuvenated high-RAP systems. Most importantly, the interaction of WVO with other modifiers such as sulfur and biochar is still not well understood, especially when it comes to simulated thermal and UV aging.

### **2.3 Synergistic or Hybrid Binder Modification Strategies**

Researchers needed to move beyond single-additive approaches given multiple and sometimes conflicting demands on asphalt pavement durability, flexibility, aging resistance, and sustainability. Waste cooking oil (WCO), sulfur, and recycled rubber are examples of individual modifiers that have shown measurable benefits in improving binder performance. However, their

limitations, such as rutting caused by softening or over-stiffening, have kept them from fully meeting the changing needs of modern pavements. In response, hybrid modification strategies that combine two or more additives have come up as a promising way to make binder systems that work well together and are balanced. These systems seek to address problems such as oxidative instability, brittleness, or poor workability by combining rejuvenators, stiffening agents, antioxidants, and nanostructured materials in a way that works together.

One of the most investigated hybrid strategies is the combination of crumb rubber (CR) and waste frying oil (WFO). The purpose of this combination is to combine WFO's ability to make HMA softer, more rejuvenating, and better flowing with CR's ability to improve elasticity and resistance to fatigue. Bilema et al. (2021) assessed RAP binders modified with both WFO and CR, noting substantial enhancements in penetration, softening point, and elastic recovery, which suggest improved resistance to oxidative aging. A study shows a nanoscale evaluation using Atomic Force Microscopy (AFM); Lyu et al. (2021) discovered that WFO minimizes the brittleness caused by rubber by softening para-phase domains and stabilizing surface morphology during both UV and thermal aging. These studies highlight the potential mechanical and microstructural enhancements achievable via WFO–CR hybrids. The performance of these systems is very sensitive to dosage, though. Most of the validation is still at the binder scale, and it's unclear how much of it applies to real-world mixture-level applications.

Sulfur-based systems have garnered significant interest owing to sulfur's ability to facilitate cross-linking and chemical stabilization. Zhou et al. (2021) looked at how sulfur interacts with bio-oil and rubberized binders. They found that crystalline cross-link formation improved the viscosity stability, softening point, and elastic recovery. Building on this idea, Mousavi et al. (2024) and Zakertabrizi et al. (2021) presented sulfur–oil hybrid systems created through inverse vulcanization, in which elemental sulfur interacts with unsaturated fatty acids (e.g., from WCO) to produce thermally stable polysulfide networks. Their research showed that sulfur radicals prefer to bind to WCO molecules that are high in alkenes. This makes a dense chemical network that is more stable against oxidative damage.

Both studies used  $\text{TiO}_2$  as a catalyst to encourage cross-linking.  $\text{TiO}_2$  made the reaction between sulfur and oil happen faster, lowered the amount of heat needed for polymerization, and kept the chemical structure stable against oxidative degradation. This dual role justifies  $\text{TiO}_2$ 's inclusion in this research: It enhances both the chemical reaction efficiency during binder formulation and the aging resistance of the final product under UV exposure, which is a critical focus of this study. Nonetheless, like most hybrid strategies, these findings are confined to binder-level assessment, and their ramifications for mixture-level performance, particularly under concurrent UV and thermal aging, remain unclear, representing a significant research gap that this thesis seeks to address.

Biochar, a porous carbonaceous substance produced from biomass pyrolysis, is being investigated increasingly in hybrid systems because it allows for numerous applications. It may serve as both a physical stabilizer and a chemical antioxidant because its surface is very porous and it has a lot of functional groups, such as hydroxyl and carboxyl. Rajib et al. (2020) showed that biochar stops UV-induced oxidative degradation by selecting free radicals and stopping the formation of carbonyl and sulfoxide groups in rubberized asphalt. Saadeh et al. (2023) expanded these findings to the mixture level, demonstrating that rubber–biochar–modified HMA mixtures significantly surpassed conventional mixtures in resistance to rutting and cracking.

Biochar has a further use in sulfur-based hybrid systems. Mousavi et al. (2024) and Zakertabrizi et al. (2021) found that biochar stabilizes sulfur-rich matrices by soaking up extra sulfur radicals and lowering the risk of over-curing, which can make materials brittle. It also helps keep sulfur in place when mixing at high temperatures and makes it easier for reactive species to spread out evenly. However, despite these findings confirming biochar's role as a UV shield and mechanical buffer, there has been no published research to date that investigates the collective efficacy of sulfur–WCO–biochar systems at the asphalt mixture level, underscoring a significant and immediate necessity for practical assessment.

Beyond sulfur–oil–carbon systems, researchers have proposed various hybrid approaches incorporating recycled plastics, fibers, and mineral additives. Zhang et al. (2022) investigated rejuvenated fiber-modified asphalt mixtures and found improved tensile strength, moisture resistance, and fatigue life. Abdelsalam et al. (2020) explored a hybrid of diatomite and lignin fibers, reporting enhanced rutting resistance without compromising flexibility. These materials act as stabilizers that reinforce binder matrices while maintaining workability.

Hybrid systems involving recycled plastic were also explored by Zakertabrizi et al. (2021), who combined WCO with recycled polyethylene and noted improved viscosity control and better resistance to oxidative aging under laboratory-simulated field aging. Likewise, Pahlavan et al. (2023) introduced bio-carbon as a carbon management strategy for HMA. Their results showed that when binder paired with sulfur, bio-carbon improved thermal stability and oxidative resistance offering an environmentally resilient binder formulation.

More nano-structural evidence was built by Lyu et al. (2023) by confirming that WFO-CR hybrid binders showed much greater resistance to nano-deformation after aging, correlating with more uniform domain distribution. According to AFM-based insights, well-designed hybrid systems could enhance macroscopic performance metrics and microstructural stability; however, most of the data stops at the binder level.

With binder-level studies attaining such a large scope, one common limitation stood out in the literature: There is an absence of mixture-level validation under realistic aging conditions. No

study has, at least within recent memory, studied this ternary system of sulfur, WCO and biochar, coupled with RAP and catalyzed by  $\text{TiO}_2$ , at the HMA mixture level. This system's response to UV and thermal aging has not been studied using important industry performance measures such as IDEAL-CT and HWT.

## **2.4 Aging Behavior and Long-Term Performance of Asphalt Mixtures**

Aging is one of the most important things that affects the durability of asphalt pavement. It changes the chemistry of the binder, the stiffness of the mixture, and the chance of cracking over time. Oxidation, hardening of the binder, and loss of flexibility happen over time when the binder is exposed to heat, oxygen, and ultraviolet (UV) radiation. To overcome these challenges, different conditioning protocols have been created to mimic field aging in the lab, both in the short and long term. The AASHTO R 30-22 standard and the NCHRP-based aging protocol created by Kim et al. (2021) are two of the most widely accepted. Thermal oxidative aging is when the binder hardens because it is exposed to high temperatures and air. This happens both during production (short-term aging) and over the life of the pavement (long-term aging). It raises the amount of asphaltene and oxygenated polar compounds, which makes the binder more viscous and less able to relax when it is under stress. This makes it more likely to crack.

To simulate long term behaviors of HMA, many researchers rely on the AASHTO R 30-22 standard, which conditions compacted asphalt specimens in a forced-draft oven at  $85 \pm 3^\circ\text{C}$  for 120 hours. This method replicates oxidative aging typically observed in the top 1–3 years of field service in dense-graded mixtures (AASHTO, 2022). While widely adopted across U.S. agencies for its standardization and ease of application, R30 has limitations, particularly its inability to produce uniform aging across the specimen depth and its insufficient representation of aging kinetics in RAP-rich or modified binders.

To overcome these shortcomings, Kim et al. (2021), through the National Cooperative Highway Research Program (NCHRP), proposed a more rigorous approach: aging loose mixtures at  $95^\circ\text{C}$  for 7 days. This method ensures uniform exposure to air and temperature, thereby producing more consistent oxidative aging throughout the material. The framework of NCHRP will also include a road-map that is regionally calibrated for the aging process, and it will try to link the thickness of the pavement and an aging duration, so that researchers might be able to realistically age field mixtures in any U.S. states. This method is increasingly preferred for long-term performance prediction, particularly in high-RAP or hybrid-modified systems where the binder's evolution over time plays a critical role in mixture behavior.

### 2.4.1. Ultraviolet (UV) Aging

Thermal aging has been a major focus of asphalt research for a long time. However, UV aging is just as important to the breakdown of the binder, especially in sunny or high-altitude areas. UV radiation starts photo-oxidative reactions that break molecular bonds and create carbonyl and sulfoxide groups. This makes the surface stiffer, more brittle, and more prone to microcracking.

Most UV aging studies are done at the binder level, using thin asphalt films under controlled laboratory irradiation, even though they are relevant to the field. Yu and Feng (2009) employed 2 mm binder films under a 500 W UV lamp at 340 nm, noting oxidation after 18 days. Hung and Fini (2020) utilized 600  $\mu\text{m}$  films subjected to UV-A radiation at 0.67  $\text{W}/\text{m}^2/\text{nm}$  for 50 hours, resulting in heightened surface roughness and the formation of oxidative byproducts. Bi and Xu (2024) and Lyu et al. (2021, 2023) investigated UV-exposed films measuring 3.0–3.2 mm, utilizing broader spectra (200–400 nm), and recorded a gradual decline in flexibility and adhesion. These studies underscore the significance of film thickness, UV wavelength, exposure duration, temperature, and photo-reactive modifiers; however, they are limited to the binder scale.

Because of this limitation, Rajib and Fini (2021) suggested a UV aging method that this study uses. Their method uses a UV irradiation chamber to mimic real-time surface degradation on several samples. It allows for even exposure, controlled film thickness, and consistent aging conditions, which makes it easier to capture surface phenomena in a more realistic way. Their research also showed that biochar that was inherently functionalized reduced oxidation and surface cracking caused by UV light, especially when used with asphalt that had rubber added to it. Rajib and Fini set the stage for testing durability in full composite systems by moving UV aging protocols to the mixture level.

Even with these improvements, there are no known studies that examined UV aging at the mixture level, especially for systems that have been changed by adding sulfur, waste cooking oil (WCO), and biochar. The functions of compaction, air voids, and aggregate–binder interaction in UV degradation remain unclear. Yet these aspects are essential because UV mostly affects the top layers of pavement, where exposure is highest and binder protection is most important.

This research directly tackles that deficiency. It uses the Rajib and Fini UV aging method on a 25% RAP mixture that has been changed with a ternary system of sulfur, WCO, and biochar, and then improved with  $\text{TiO}_2$ . The goal is to determine how thermal and UV aging together affect cracking and rutting resistance, as measured by IDEAL-CT and HWT. This integrated approach provides one of the initial insights into mixture-level UV degradation in sustainable, high-RAP asphalt systems, aiding in future material selection and design methodologies.

## 2.5 Testing Protocols and Performance Evaluation

Mechanical tests that simulate common pavement problems such as cracking and rutting are the traditional way of testing the behavior of asphalt mixtures. A crucial step in selecting appropriate performance tests is determining how modified binders, aging conditions, and recycled content influence long-term pavement behavior. The two widely applied well-established standards tests relevant for asphalt mixtures, particularly those containing significant quantities of RAP and additives, are the IDEAL-CT for cracking and the HWT Test for rutting.

Cracking is typical with common asphalt pavements, especially in areas with a lot of traffic and changes in temperature. The IDEAL-CT, which is standardized under ASTM D8225, is known for being simple, repeatable, and effective in measuring the likelihood of compacted asphalt specimens cracking. It measures two parameters that are highly susceptible to changes in binder stiffness, mixture composition, and aging condition: fracture energy ( $G_f$ ) and the Cracking Tolerance Index ( $CT_{index}$ ).

Among the significant advantages of IDEAL-CT is that it needs no notching or any other sample preparation that would involve time and expenses, unlike classic fracture tests such as Semi-Circular Bend or Disk-Shaped Compact Tension. In research settings, SCB and DCT might still be considered valid approaches. IDEAL-CT, however, has demonstrated rapid growth in credibility and acceptance and, therefore, has been incorporated into DOT-level specifications for performance-based mix designs.

IDEAL-CT was noted by researchers to help in assessing the modification effects on cracking resistance and the aging protocol. For instance, long-term exposure to thermal or UV demonstrated a decline in  $G_f$  and  $CT_{index}$  after oven aging. Consequently, IDEAL-CT is very well suited to evaluate cracking susceptibility in hybrid-modified, high-RAP systems where the stiffness and ductility trade-off is critical for long-term durability.

Increased stiffness with aging reduces cracking to some extent, but it may also improve rutting resistance. Hence, rutting performance needs to be tested independently, thus making sure a proper balance of mixture properties. The HWT test, as described in AASHTO T 324, finds wide acceptance as a rutting deformation and moisture susceptibility test under submerged and repeated load conditions. HWT is particularly advantageous in evaluating modified binders and high-RAP mixtures where stiff binder matrices may mask moisture-related damage or deformability under load. The test simulates wheel tracking under a 50°C water bath, and rut depth is recorded over 20,000 cycles (or more), providing a clear indication of the mixture's ability to resist permanent deformation and stripping.

The sensitivity of HWT to binder stiffness, aggregate structure, and modifier type makes it a valuable complement to IDEAL-CT. While some alternatives such as the Flow Number test or

Asphalt Pavement Analyzer (APA) exist, HWT is generally favored for its dual assessment of rutting and moisture resistance in a single setup. Recent literature has demonstrated that mixtures aged under both thermal and UV protocols often experience changes in rutting performance, with modifiers such as sulfur, rubber, or biochar enhancing or degrading resistance depending on dosage and interaction effects.

Integrating the results of IDEAL-CT and HWT to assess cracking and rutting resistance of HMA provides a balanced performance assessment with respect to aging effect. Such a dual-test strategy proves to be important when assessing modified asphalt systems that undergo long-term thermal and ultraviolet aging, where competing phenomena of binder hardening and embrittlement must be considered simultaneously.

These tests have more importantly been successfully applied in the literature with a variety of materials and aging conditions, including high-RAP mixtures, bio-based modifiers, and hybrid additive systems, meaning that they also fit well for the characterization of advanced, sustainable pavement solutions.

This chapter reviewed the current state of knowledge on sustainable asphalt modifiers, reclaimed asphalt pavement (RAP) rejuvenation, hybrid binder systems, aging mechanisms, and relevant performance testing protocols. The literature reveals that while bio-based additives such as WCO, sulfur, and biochar have shown promising results, particularly at the binder level, their combined effects under long-term thermal and UV aging at the mixture level remain largely unexplored. Furthermore, existing UV aging studies only focus on binder level; therefore, the complex behavior of HMA is disregarded. Finally, the IDEAL-CT and HWT tests have emerged as practical, reliable tools for capturing aging-related damage. These gaps justify the current study's aim to evaluate a ternary-modified high-RAP asphalt mixture subjected to combined aging conditions, with the goal of advancing sustainable and durable pavement design.

### 3. Objective

The primary objective of this study is to assess the performance of RAP asphalt mixtures produced with a binder modified using sulfur, waste cooking oil (WCO), and biochar. These low-carbon modifiers, together with RAP, contribute to improving the long-term sustainability and durability of asphalt mixtures. The multi-additive system composed of sulfur, waste cooking oil (WCO), and biochar at a ratio of 2:4:1 is expected to enhance cracking and rutting resistance while reducing the environmental impacts associated with conventional asphalt production. This research uses a control mixture containing 25% RAP and compares it to mixtures made with binder modified by 10% and 20% total additive content (by binder weight). In addition, titanium dioxide (TiO<sub>2</sub>) at 0.08% by sulfur weight is used to enhance the performance and aggregate-binder bond in mixture.

To simulate field aging, specimens were subjected to thermal aging at 3, 5, and 7 days (representing 4, 8, and 10 years of field aging in Southern California, respectively, based on NCHRP Research Report 973). An additional set underwent 3 days of thermal aging and UV aging for 72 hours based on the aging protocol of Rajib and Fini (2020). These combinations represent a comprehensive factorial design, shown in Table 1.

To evaluate the performance of the mixtures, two key laboratory tests were conducted:

- Indirect Tensile Asphalt Cracking Test (IDEAL-CT) to evaluate fracture resistance and cracking susceptibility.
- Hamburg Wheel Tracking (HWT) test to determine rutting resistance under wet and repeated loading conditions.

These tests were used to compare the long-term cracking and rutting resistance of mixtures containing low-carbon sulfur polymer modifiers at two dosage levels (10% and 20%) with that of the control mixture. The experimental program also aimed to assess the resistance of the modified mixtures under different thermal and UV aging conditions; evaluate the combined effects of biochar, waste cooking oil, and sulfur on aging durability; and determine the optimal additive content that improves sustainability and mechanical performance without compromising durability.

Table 1. Test Factorial

HMA Mixture	Aging Level	Sample Identification
Control Mix	Without Aging	CM-WA
	3 days	CM-3d
	5 days	CM-5d
	7 days	CM-7d
	3 days thermal aging + 3 days UV aging	CM-UV
Control mix with Biochar, Waste Cooking Oil, and Sulfur (1:4:2) 10% of Total Weight of binder	Without Aging	10%-WA
	3 days	10%-3d
	5 days	10%-5d
	7 days	10%-7d
	3 days thermal aging + 3 days UV aging	10%-UV
Control mix with Biochar, Waste Cooking Oil, and Sulfur (1:4:2) 20% of Total Weight of binder	Without Aging	20%-WA
	3 days	20%-3d
	5 days	20%-5d
	7 days	20%-7d
	3 days thermal aging + 3 days UV aging	20%-UV

## 4. Materials

This chapter summarizes the materials used in preparing the Hot Mix Asphalt (HMA) mixtures evaluated in this study. All materials were selected to reflect typical Southern California paving conditions, based on Caltrans standards, with a focus on sustainability and long-term performance.

### 4.1. Aggregate

Aggregates made up 90–95% of the total mix weight and provided the structural skeleton of the pavement. The aggregates were sourced from Vulcan Materials Company – Corona Drum Plant, and their gradation followed the specifications for ¾" HMA Type A shown in Figure 1. The design gradation ensured good interlock, workability, and durability.

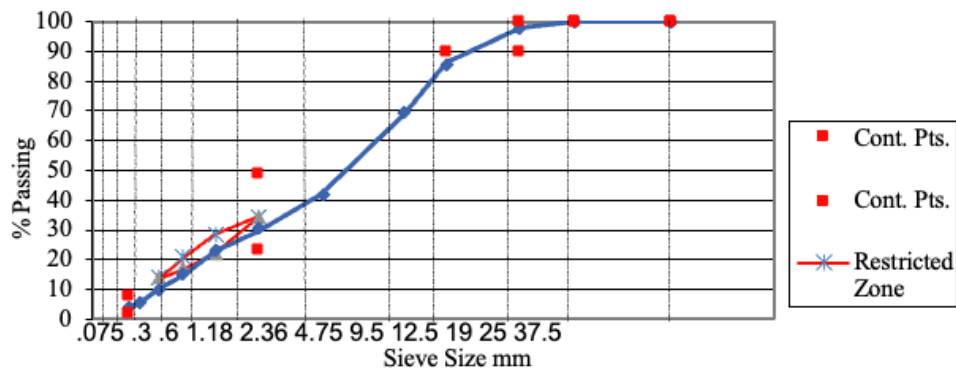
### 4.2 Asphalt Binder

All mixtures used a PG 58-16 asphalt binder supplied by San Joaquin Refining Co., Inc. This binder was selected for its compatibility with regional climate conditions. For modified mixtures, a low-carbon additive blend consisting of sulfur, waste cooking oil (WCO), and biochar was introduced at two dosage levels: 10% and 20% by binder weight, in a 1:4:2 ratio. Additionally, TiO<sub>2</sub> was added by 0.08% of sulfur weight to enhance binder-aggregate bonding. Binder properties are shown in Table 2.

### 4.3 Reclaimed Asphalt Pavement (RAP)

To improve sustainability, 25% RAP was used in all mixtures. The RAP was screened, processed, and blended with virgin aggregates, as specified in the Job Mix Formula (JMF). Its binder content and gradation were within Caltrans tolerances and consistent with the mix design.

Figure 1. Aggregate Gradation Curve



#### **4.4 Additives**

To enhance sustainability and improve aging resistance, a combination of biochar, waste cooking oil (WCO), and sulfur was used as a low-carbon additive system. These additives were blended at a ratio of 1:4:2 by weight and incorporated at two dosage levels, corresponding to 10% and 20% of the total binder weight. Each component served a specific role in modifying the binder properties. Sulfur was primarily included to improve high-temperature performance and increase rutting resistance through the formation of a sulfur-based polymer network. Waste cooking oil acted as a rejuvenator by restoring binder flexibility and improving workability, particularly in RAP mixtures where aged binder tends to be stiff and brittle. Biochar contributed to enhanced aging resistance and UV protection due to its high carbon content and porous structure, while also facilitating interaction between sulfur and WCO within the modified binder system. In addition, titanium dioxide ( $\text{TiO}_2$ ) was incorporated at 0.08% by weight of sulfur to enhance aggregate–binder bonding within the mixture.

Table 2. Asphalt Binder Properties

Property	Test Method	Results (PG 58-16)	Spec Limit
<b>Binder Identification &amp; Composition</b>			
Asphalt Binder Grade	AASHTO M320	PG 58-16	PG 58-16
Asphalt Binder Content (%)	AASHTO T308	4.70%	4.5–5.2% (typical)
RAP Binder Content (%)	ASTM D2172	4.77%	N/A
<b>Original Binder Properties</b>			
Flash Point (°C)	ASTM D92 / AASHTO T48	302	≥230
Viscosity @ 135°C (Pa·s)	ASTM D4402 / AASHTO T316	0.255	≤3.0
G*/sin(δ) @ 58°C (kPa)	AASHTO T315	1.742	≥1.00
Phase Angle, δ (°)	AASHTO T315	88.79	–
<b>RTFO Aged Binder Properties</b>			
Mass Loss (%)	AASHTO T240	-0.085	≤1.00
G*/sin(δ) @ 58°C (kPa)	AASHTO T315	3.501	≥2.20
Phase Angle, δ (°)	AASHTO T315	87.44	–
<b>PAV Aged Binder Properties</b>			
G*·sin(δ) @ 25°C (kPa)	AASHTO T315	4300	≤5000
Phase Angle, δ (°)	AASHTO T315	57.31	≥42°
BBR Test @ -6°C	AASHTO T313		
Stiffness, S (MPa)	AASHTO T313	77.5	≤300
m-value	AASHTO T313	0.439	≥0.300
<b>Other Properties</b>			
Specific Gravity @ 60°F	ASTM D70	1.0154	–

## 5. Methodology

This chapter describes the process by which the hot mix asphalt (HMA) mixtures used in this study were made, modified, aged, and tested. The methodology was developed to replicate actual aging conditions and assess both fracture and rutting performance in laboratory-controlled environments. A factorial experimental methodology was utilized to investigate the synergistic effects of low-carbon modifiers and thermal/UV aging over time. The experimental plan included three types of asphalt mixtures: a control mixture (CM) with 25% reclaimed asphalt pavement (RAP) and two modified mixtures with 10% and 20% low-carbon modifier content (by binder weight). The additives were a mix of sulfur, waste cooking oil (WCO), and biochar in an ordered ratio of 1:2:4. All mixtures were aged for a short time and then put through different long-term aging conditions (3, 5, and 7 days) or a combination of thermal and UV aging, as explained in Chapter 3.

### 5.1 Mixing and Sample Preparation

The approved Job Mix Formula (JMF) indicated that the mixtures should have 25% reclaimed asphalt pavement (RAP). The control mixture (CM) has an optimum binder content at 4.7% PG 58-16 asphalt binder by total weight, provided by Vulcan Material Company. Similar optimum binder content of 4.7% was found for the 10% modified mixture; however, the 4.6% optimum binder content was found for the 20% modified mixture. To ensure the coating and workability were correct, all mixing tools, including the mixing bucket, mixer paddles, and spatulas, were heated to 162°C (325°F) for at least two hours.

Figure 2. Shear Mixer Used for This Project



The first stage in mixing is to heat the aggregates and transfer them to a heated bucket. After that, the right amount of PG 58-16 binder was added to the aggregate. For the modified binders, biochar, sulfur, and waste cooking oil (WCO) were mixed together in a ratio of 1:2:4. Before being mixed with the binder, sulfur was heated to 160°C to make it softer. It was then mixed with biochar in a 2:1 ratio and left in the oven for 30 minutes at 160°C to make sure the chemical process was completed. After the binder reached the proper temperature for mixing, the biochar with WCO and sulfur in a 1:4:2 was added to it. A laboratory shear mixer was used to mix the two together at 400 rpm for 18 minutes (Figure 2). Also, we added titanium dioxide (TiO<sub>2</sub>) at 0.08% of the weight of sulfur to help the reaction between sulfur and WCO. To wrap up the chemical integration process, the final modified binder was put in an oven at 160°C for an hour.

Figure 3. Control Mix After Short-Term Aging



After the binder was ready, the modified or control binder was added to the preheated aggregates and mixed with a mobile mixer, as shown in Figure 4, until the coating was complete. According to AASHTO R30, the loose HMA was aged for two hours at 135°C in an oven after it was mixed. Figure 3 shows the mixture after the short-term aging. After an hour, the mixture was stirred to make sure it heated evenly. After it had aged, the mix was spread out on trays that were 1 to 2 inches thick so that it could cool and be tested again. Five different levels of aging were used to simulate the field's aging at five distinct stages of the pavement's service life. There were 60 samples made for the Hamburg Wheel Tracking Test and 45 samples made for the IDEAL

Cracking Test. After these steps were taken to get ready, all the tests were done according to the experimental protocol.

Figure 4. Mobile Mixer to Mix Aggregates with Binder



## 5.2 Aging

The long-term aging process in this study aimed to determine whether modified hot mix asphalt (HMA) mixtures withstand conditions that mimic real-world aging. The mixtures were aged for 3, 5, and 7 days at 95°C, a protocol specified for the Long Beach region as outlined in the NCHRP Research Report 973. The NCHRP Research Report 973 gives guidelines for the period that laboratory aging should last and maps based on historical pavement temperature data from different places in the United States that was collected using the Enhanced Integrated Climatic Model (EICM). The aging times were picked to represent different stages of the life of the pavement: Aging for 3 days corresponds to aging for 3–5 years in service, 5 days is comparable to aging for 7–10 years, and 7 days represented aging for 12–15 years at a depth of 6 mm. This method ensures that the aging process accurately mimics the physical changes and oxidative hardening that the pavement will likely go through over time.

To get even aging throughout the material, loose mix aging was used instead of compacted mix aging. When specimens are compacted, aging mostly happens on the surface, which may not be an accurate methodology to predict how the mix will perform over time. The loose mix method lets oxygen get in more evenly, resulting in a more realistic simulation of field conditions. This method is crucial for modified mixtures containing biochar, sulfur, and waste cooking oil. Since these additives may react differently with the binder during aging, a baseline condition without long-term aging was established; therefore, the mixtures were subjected only to short-term

aging. This baseline was set up to assess how the mixtures perform in the early stages and how they change over time. The short-term aging was done at  $135 \pm 3^\circ\text{C}$  for 2 hours, following AASHTO R 30-22, ensuring the samples were ready for performance testing promptly. Adding this baseline makes it easy to examine how the mixtures change from their initial state to their long-term performance. This comprehensive method gives useful information about the long-term and short-term performance of the modified HMA mixtures.

A UV aging procedure was used to simulate the effects of ultraviolet radiation on modified HMA mixtures, in addition to the long-term aging methods. This process followed the procedures set out by Rajib et al. (2020), which gives a structured way to age bituminous materials using UV light. The modified mixtures were first put through 3 days of normal aging at  $95^\circ\text{C}$  to make sure they all started from the same point, which resembles the first few years of long-term field exposure. After the 3-day aging process was done, the samples were moved to a UV chamber to accelerate the aging process. The UV chamber used in this study was designed to simulate intense sunlight. The chamber has a controlled environment with a radiation intensity of  $13.6 \text{ W/m}^2$  at a wavelength of 315–400 nm. This is a common setting used to simulate the effects of long-term exposure to sunlight. The specimens were put 15 to 18 cm away from the UV lamp and left there for 72 hours. The temperature in the chamber remained at an average of  $40^\circ\text{C}$  throughout, and the temperature of the loose mixture surface ranged between 50 and  $55^\circ\text{C}$ . The humidity was also measured at 27%. Figure 5 shows how to set up the UV aging chamber.

This method ensured that UV penetration was consistent, affecting both the surface and subsurface layers of the HMA mixtures. This is important for measuring UV-induced oxidative changes. The reason for this two-step aging process, which began with three days of thermal aging and concluded with 72 hours of UV exposure, was to accurately simulate the effects of heat and sunlight on the pavement over its lifetime. UV radiation is known to make free radicals form more quickly in the binder, resulting in more brittleness and cracks (Rajib, 2020). The study sought to deliver a thorough comprehension of the performance of modified HMA mixtures, especially those incorporating biochar, sulfur, and waste cooking oil, under the influence of concurrent oxidative and UV stresses. This method not only helps figure out how long-lasting the mixtures are, but it also shows how well they can resist common aging processes, making pavement infrastructure last longer.

Figure 5. UV Chamber



### 5.3 Compaction and Fabrication

The specimens required for this study were prepared according to Table 1 of Chapter 3. The compacted samples should have a diameter of 150 mm and a thickness of 62 mm, and three replicates were tested for the IDEAL CT. Four specimens with a thickness of 60 mm were prepared for each aging level, forming two sets of samples for the HWT test. The volumetric tests used to prepare the samples with those specifications are listed below:

- AASHTO T 209: Standard Method of Test for Theoretical Maximum Specific Gravity (Gmm)
- AASHTO T 312: Preparing and Determining the Density of Asphalt Mixture Specimens using the Superpave Gyratory Compactor
- AASHTO T 166: Bulk Specific Gravity (Gmb) of Compacted Asphalt Mixtures Using Saturated Surface-Dry Specimens
- AASHTO T 269: Standard Method of Test for Percent Air Voids in Compacted Dense and Open Asphalt Mixtures.

For determining the theoretical maximum specific gravity (Gmm) of the mixtures, as explained in AASHTO T209, the first step is to conduct a test. The NMAS for this mix is 19 mm, and each mixture requires 2200 gm. For measuring Gmm, the loose mix is used; large particles must be carefully separated or divided by hand without breaking them or getting any binder stuck to the container or hands. The fine aggregate part should be no more than a quarter of an inch thick. Initially, water at 25°C was placed in the pycnometer, and its weight was measured. After that, the pycnometer was emptied and the sample was put inside. It was then put back in the water at 25°C. A vacuum pressure of  $27.5 \pm 2.5$  mmHg was maintained for 15 minutes, while a mechanical shaker kept the mixture moving. This pushed the air pockets out and replaced them

with water. Figure 6 shows the tools that were used for this test. After 15 minutes, the pressure was released at a rate of no more than 60 mmHg per second. When the atmospheric pressure was proper, the pycnometer was partially filled with water, and the samples were completely filled with water. Lastly, we weighed the pycnometer and the sample, and then equation 1 was used to determine the mix's Gmm.

$$G_{mm} = \frac{A}{A+D-E}$$

Where:

$G_{mm}$  = theoretical maximum specific gravity.

A = mass of oven-dry sample in air (g).

D = mass of pycnometer filled with water at 25°C (g).

E = mass of pycnometer filled with the sample and water at 25°C (g).

Figure 6. Vacuum Saturation of Conditioned Loose Asphalt Mixture and Shaker



To determine the bulk specific gravity, the mixture was compacted using the Superpave Gyratory Compactor in accordance with AASHTO 312. A Superpave Gyratory Compactor was used to compact all of the specimens according to AASHTO T 312-22, which explains how to use the Superpave method to compact asphalt mixture specimens. The compactor, shown in Figure 7, performed at a pressure of  $600 \pm 18$  kPa, a gyration angle of  $1.16 \pm 0.02$  degrees, and a compaction rate of  $30 \pm 0.5$  gyrations per minute and 5 minutes of squaring time for specimens to cool down. Before compaction, the mold, end plates, and other parts were heated up for at

least 30 minutes. After short-term aging was done, the asphalt mixtures were compacted while they were still hot. The cylindrical specimens were compacted to a diameter of 150 mm and a target thickness of 62 mm and 60 mm, making them suitable for both the IDEAL-CT and the Hamburg Wheel Tracking Test, which needed a thickness of 60 mm. We weighed each batch of mixture to make sure that all the specimens had a comparable mass. To keep the samples from sticking to the compaction plates, paper discs were put at the top and bottom of each one. The temperature for compaction was kept between 131 and 135°C, which is within the recommended range for PG 58-16 binders.

After being compacted, the samples were left to cool to room temperature, either overnight or with the assistance of a fan, depending on the scheduled test time. Any samples that were too thick or too thin or that did not look good were thrown away and replaced.

The bulk specific gravity ( $G_{mb}$ ) of the compacted specimens was determined using the saturated surface-dry (SSD) method in accordance with AASHTO T 166-22. The procedure requires measuring the specimen in three weight conditions:

A: Mass of the dry specimen in air, (g).

B: Mass of the SSD specimen in air, (g).

C: Mass of the specimen submerged in water, (g).

The  $G_{mb}$  was calculated using the following equation:

$$G_{mb} = \frac{A}{B - C}$$

Before weighing, the sample was placed in an SSD state by immersing it in water and then drying its surface with a damp cloth to remove any excess moisture. The weighing was done quickly; otherwise, the sample could have dried out while being weighed. All specimens were tested to ensure the results agreed among them. Afterward, since air void content in each sample was calculated using the measured  $G_{mb}$  values and the theoretical maximum specific gravity ( $G_{mm}$ ), which was determined by following AASHTO T 209 procedures, these volumetric parameters allowed us to evaluate the consistency of the mixture and the process of compaction. They also helped determine the effect of both the quantity of additives and the age of the mixture on its performance.

Figure 7. Superpave Gyrotory Compactor for Specimen Compaction



After determining the  $G_{mm}$  and  $G_{mb}$ , the AASHTO T 269 test was implemented to determine the air void. AASHTO T 269 is used to find the percentage of air voids ( $P_a$ ) in the compacted asphalt mixtures. This is the standard way to find the percentage of air voids in dense and open-graded asphalt mixtures. The air void content is the amount of air pockets left in the compacted mix. It is an important factor in determining how strong and dense the pavement is. Using the SSD method (AASHTO T 166), we found the bulk specific gravity ( $G_{mb}$ ) for each specimen. Then, using AASHTO T 209, we found the theoretical maximum specific gravity ( $G_{mm}$ ) for each specimen. The percentage of air voids was then found using the following formula:

$$P_a = 100 * \left(1 - \frac{G_{mb}}{G_{mm}}\right)$$

$P_a$  = percent air voids

$G_{mb}$  = bulk specific gravity of the compacted specimen

$G_{mm}$  = theoretical maximum specific gravity of the mix

The calculated  $P_a$  values were rounded to one decimal place as per specification. These values were used to confirm that all compacted samples achieved the target range of  $7.0 \pm 0.5\%$  air voids, in accordance with Superpave mix design requirements. Any specimen falling outside of this tolerance was excluded from performance testing.

## 6. Testing Method

This study investigates the rutting resistance and fatigue cracking resistance of asphalt mixtures along with a multi-modifier system, at five different aging levels. The compacted samples were examined using the following method:

ASTM D8225: Standard Test Method for Determination of Cracking Tolerance Index of Asphalt Mixture Using the Indirect Tensile Cracking Test at Intermediate Temperature.

AASHTO T 324: Standard Method of Test for Hamburg Wheel-Track Testing of Compacted Asphalt Mixtures.

### 6.1. Indirect Tensile Asphalt Cracking Test

The Indirect Tensile Cracking Test at Intermediate Temperature was conducted in the first part of this study according to the ASTM D8225-19 standard, for which an indirect tensile loading frame was attached to the Dynamic Testing System (DTS), manufactured by Pavetest (FIGURE 8). The DTS machine is composed of an axial loading device, a load cell, loading strips, a sample deformation measurement device, temperature-controlled chambers, and a data control and acquisitions system. The test comprises a minimum of three samples compacted in a Superpave gyratory compactor (SGC), with a diameter of 150 mm and 62 mm thick. For samples with a diameter of 150 mm, the loading strip must be 19.05 mm wide, while the length should be greater than the thickness of the sample. The compacted samples should not be notched, cut, glued, or drilled, thereby simplifying sample fabrication.

The  $CT_{index}$ , which measures the fatigue cracking resistance, is a fracture-mechanics-based parameter. The  $CT_{index}$  is calculated by taking into account the failure energy, the post-peak slope of the load-displacement curve, and the deformation tolerance at 75% of peak load. Higher values of  $CT_{index}$  indicate superior cracking resistance of the sample. The fatigue cracking resistance tests were conducted at a room temperature of 25°C, which is based on the calculated temperature based on the specification and equation below.

$$PG\ IT = \frac{PG\ HT - PG\ LT}{2} + 4$$

Where:

PG IT = intermediate performance grade temperature (°C),

PG HT = climatic high-performance grade temperature (°C), and

PG LT = climatic low-performance grade temperature (°C).

To conduct the test, the temperature chamber was set at 25°C, and, upon temperature stabilization, the compacted samples were placed inside the chamber for 2 hours ± 10 minutes. The indirect tensile frame's contact surface must be cleaned so that it is free from debris since any debris may affect the measurement. The samples were then inserted inside the DTS testing machine, fitting inside the indirect tensile loading frame. The samples are centrally placed in the jig to make uniform contact with the supports. The input parameters of 50 mm/minute loading rate and 0.1 kN termination load were entered into the software for the start of the test. For each sample/test, the software recorded displacements and the corresponding loads. The test would stop once the compacted sample was considered failed. When displacement took place under a load less than 0.1 kN, the sample was declared to have failed. The load was then plotted versus displacement. Each test produces a load vs displacement curve. The area under the load vs displacement curve through the quadrangle rule provides work of failure  $W_f$  as shown in equation 1.

$$W_f = \sum_{i=1}^{n-1} ((l_{i+1} - l_i) \times P_i + \frac{1}{2} \times (l_{i+1} - l_i) \times (P_{i+1} - P_i)), \text{ where}$$

(1)

$W_f$  = work of failure (joules),

$P_i$  = applied load (kN) at the  $i^{th}$  load application,

$P_{i+1}$  = applied load (kN) at the  $(i^{th} + 1)$  load application,

$l_i$  = LLD (mm) at the  $i^{th}$  step, and

$l_{i+1}$  = LLD (mm) at the  $i^{th}$  step.

Another parameter required to determine  $CT_{index}$ , failure energy  $G_f$ , can be calculated with the help of the work of failure  $W_f$ . Failure energy  $G_f$  can be calculated by dividing  $W_f$  by the cross-sectional area of the sample, as shown in equation 2:

$$G_f = \frac{W_f}{D \times t} \times 10^6, \text{ where: (2)}$$

$G_f$  = failure energy (joules/ $m^2$ ),

$W_f$  = work of failure (joules),

D = sample diameter (mm), and

t = sample thickness (mm).

The final parameter, post-peak slope ( $m_{75}$ ), is the slope of the tangential zone around the 75% peak load point after the peak.

$m_{75}$  can be calculated using equation 3:

$$|m_{75}| = \left| \frac{P_{85} - P_{65}}{l_{85} - l_{65}} \right|, \text{ where:}$$

(3)

$P_{85}$  = 85% of the peak load (kN) at the post-peak stage,

$P_{65}$  = 65% of the peak load (kN) at the post-peak stage,

$l_{85}$  = displacement (mm) corresponding to 85% of the peak load at the post-peak stage,  
and

$l_{65}$  = displacement (mm) corresponding to 65% of the peak load at the post-peak stage.

Finally, after calculating these parameters, the  $CT_{index}$  can be determined using equation 4:

$$CT_{index} = \frac{t}{62} \times \frac{l_{75}}{D} \times \frac{G_f}{|m_{75}|} \times 10^6$$

Where: (4)

$CT_{index}$  = failure energy (joules/ $m^2$ ),

$G_f$  = failure energy (joules/ $m^2$ ),

D = sample diameter (mm),

$|m_{75}|$  = absolute value of the post-peak slope  $m_{75}$  (N/m),

$l_{75}$  = displacement at 75% of the peak load after the peak (mm), and

t = sample thickness (mm).

The  $CT_{index}$  was calculated for each sample and prepared for statistical analysis. The load-displacement graphs, along with the parameters of the  $CT_{index}$ , are listed in the results portion of this thesis.

Figure 8. DTS Machine for IDEAL-CT Testing



## 6.2. Hamburg Wheel Tracking Test

AASHTO T 324-22 describes the Hamburg Wheel Tracking (HWT) Test to assess the material resistance to rutting and moisture sensitivity. This method requires repeatedly loading submerged HMA samples with a steel wheel that moves back and forth while the temperature is kept at a certain level. The test gives us important information about how well the mixture can resist permanent deformation and how likely it is to be damaged by moisture. The test was done with the Cox Hamburg Wheel Tracker, which is an electric device with two steel wheels that are  $203.2 \pm 2.0$  mm (8 in.) in diameter and  $47 \pm 0.5$  mm (1.85 in.) in width. Each wheel puts a load of  $703 \pm 4.5$  N on the specimens and moves back and forth over the center of the specimens  $52 \pm 2$  times per minute, like traffic does. The wheels move in a sinusoidal pattern across the surface of the specimen, which makes sure that the load is even. We used the Superpave Gyratory Compactor (SGC) to compact all of the specimens, and then we saw-cut them (FIGURE 9) to a thickness of 60 mm in the G3 quality lab.

For each test, four cylindrical specimens with a diameter of 150 mm were made and put in two pairs in the stainless-steel mounting tray. The mounting system was made to hold the specimens in place and let at least 20 mm of water flow around each sample while testing. High-density polyethylene (HDPE) molds were used to mount the specimens, making sure they stayed in place

during the test. The test chamber was filled with water, and the temperature was set and kept at  $50^{\circ}\text{C} \pm 1.0^{\circ}\text{C}$ , which was based on the binder's performance grade (PG 58-16). After being submerged, the specimens were preconditioned for 20-30 minutes to reach thermal equilibrium before being loaded. Then, testing began using the device's software in automatic mode.

The test was configured to terminate upon reaching either a maximum rut depth of 20 mm or 20,000 passes, whichever occurred first. The linear displacement transducer (LDT) recorded the rut depth at multiple intervals, and the software continuously plotted rut depth versus number of passes. In addition, the Stripping Inflection Point (SIP) was identified as the point at which the rate of deformation sharply increased due to moisture-induced debonding of the binder from the aggregates. The final rut depths were calculated by averaging the maximum deformation from both specimen pairs.

This procedure allowed for a reliable and standardized assessment of the long-term rutting performance and moisture resistance of both the control and modified HMA mixtures under simulated field conditions.

Figure 9. Hamburg Wheel Track Test Setup After Test



## 7. Results and Analysis

### 7.1 Hamburg Wheel Tracking Test

The Hamburg Wheel Tracking (HWT) test was performed according to AASHTO T 324 to assess the material resistance to rutting and moisture sensitivity. All specimens were compacted to a height of 60 mm and a diameter of 150 mm. Prior to testing, the specimens were placed in a 50°C water bath for 20 to 30 minutes to ensure they were all at the same temperature, to simulate real-life conditions. Testing was performed at 50°C with a typical steel wheel load, and rutting measurements were collected up to 20,000 passes.

The HWT test, according to AASHTO T 324, measures rut depth up to 20,000 passes. However, this study used rutting values at 15,000 passes to compare the extent to which the mixture performed. This mid-cycle comparison method makes it easier to identify early signs of rutting, especially for mixtures that did not fail or show stripping inflection points (SIP) during the entire test. Also, several transportation agencies, such as Caltrans and TxDOT, have set rutting thresholds (e.g., 12.5 mm) at 15,000 passes, which indicates that this evaluation interval stays valuable.

Table 3 and Figure 10 demonstrate the final rut depths measured after 15,000 passes for the control mixture (CM) and the mixtures with 10% and 20% of the modifier (biochar, WCO, sulfur) over different amounts of aging. All specimens remained well below the normal failure point, allowing for a comparison of their relative performance across different aging conditions and modifier dosages. The HWT test results indicated that the rut depth always became shallower as the pavement aged, which means that rutting mostly happens in the early stage of a pavement's life. As mixtures age thermally, the oxidation of the binder makes them stiffer, which makes them less likely to change shape permanently. Notably, modified mixtures with 10% and 20% low-carbon sulfur polymer additives showed better rutting resistance than the control mix, especially after being aged for a long time. The only exception is 20%-WA, which shows significant rut depth, more than 20 mm, after around 6,000 passes. After 7 days of aging, both modified mixtures had shallower average rut depths than the control. The 20% dosage was the most resistant. This trend indicates that the modifiers positively impact long-term pavement performance by increasing stiffness without reducing durability. The fact that there are no sudden changes in slope or inflection points shows that all mixtures except 20%-WA are stable when they are loaded repeatedly. These results support the idea that the proposed sustainable additives might serve as effective replacements for typical binders, especially in situations where more durability and environmental performance are needed.

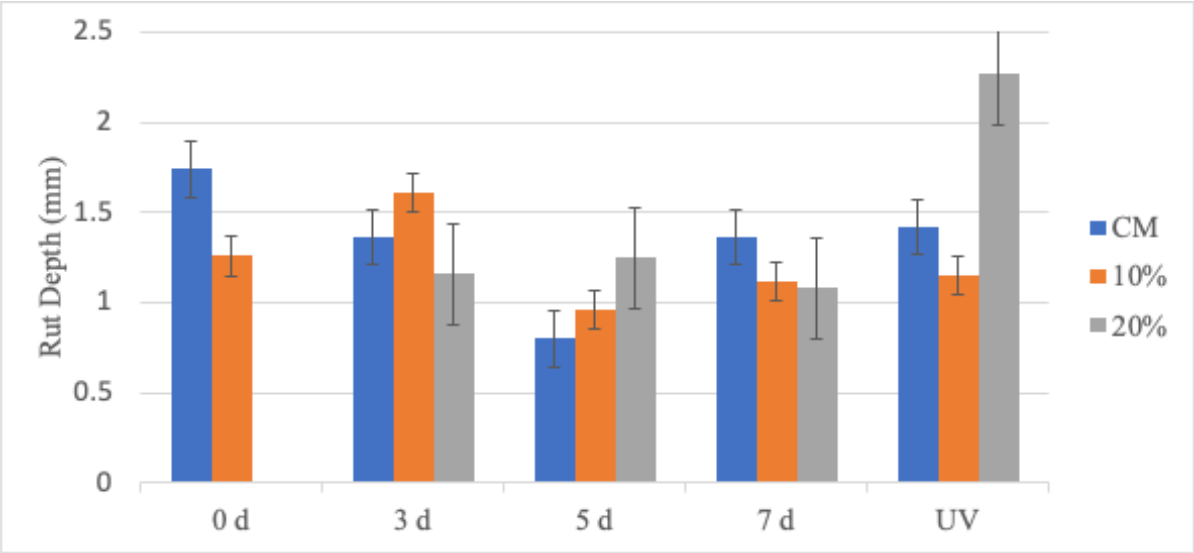
Table 3. Hamburg Wheel Rut Depth Results at 15,000 Passes

Aging Level	Sample ID	Rut Depth (mm)			Stripping Inflection Point
		Side 1	Side 2	Average	
Without Aging	CM-WA	-2.16	-1.33	-1.75	N/A
	10%-WA	-2.06	-0.45	-1.26	N/A
	20%-WA	N/A*	N/A*	N/A*	N/A
3 days	CM-3d	-0.58	-2.13	-1.36	N/A
	10%-3d	-2.35	-0.87	-1.61	N/A
	20%-3d	-2.03	-0.29	-1.16	N/A
5 days	CM-5d	-1.33	-0.27	-0.80	N/A
	10%-5d	-0.96	-0.95	-0.96	N/A
	20%-5d	-1.86	-0.64	-1.25	N/A
7 days	CM-7d	-2.44	-0.27	-1.36	N/A
	10%-7d	-0.97	-1.28	-1.13	N/A
	20%-7d	-1.87	-0.28	-1.08	N/A
UV	CM-UV	-1.89	-0.95	-1.42	N/A
	10%-UV	-0.62	-1.42	-1.02	N/A
	20%-UV	-1.76	-2.74	-2.25	N/A

N/A\*: Values for the 20%-WA mixture are not reported due to the observed significant rut depth after only 6,000 passes.

This mix exhibited excessive rutting beyond expected limits, and the data were excluded from analysis to maintain consistency and reliability of the results.

Figure 10. Average Rut Depth at 15,000 Passes



Note: Values for the 20%-WA mixture are not reported due to observed inconsistencies during testing. This mix exhibited excessive rutting beyond expected limits, and the data were excluded from analysis to maintain consistency and reliability of the results.

Figures 11 through 15 illustrate the average rut depth as a function of the number of passes for asphalt mixtures that underwent different aging protocols: without aging, thermal aging (for 3, 5, and 7 days), and a combination of thermal and UV aging. In the unaged condition, the control and both modified mixtures (10% and 20%) exhibited a comparable rutting pattern, with the 10% modified mix demonstrating a marginally reduced rut depth overall. After three days of thermal aging, there was no obvious ranking of the mixtures' performance. However, the 20% mix performed better than the control and 10% mixes. After 5 days of aging, the 20% modified mixture exhibited significantly more rutting than the 10% mixture, which remained close to the control. After 7 days, all of the mixtures showed the same rutting behavior, which means that the stiffening effect from aging had made it less likely for them to deform further. The 10% modified mixture was the most resistant to rutting when exposed to UV aging (thermal + UV). The 20% mix had the deepest rut depth in all conditions. None of the curves showed sudden changes in slope in any of the scenarios. This means that there was no moisture damage or stripping, and it suggests that the rutting resistance stays the same as the aging levels go up.

Figure 11. Rut Depth vs No. of Passes for Mixtures Without Aging

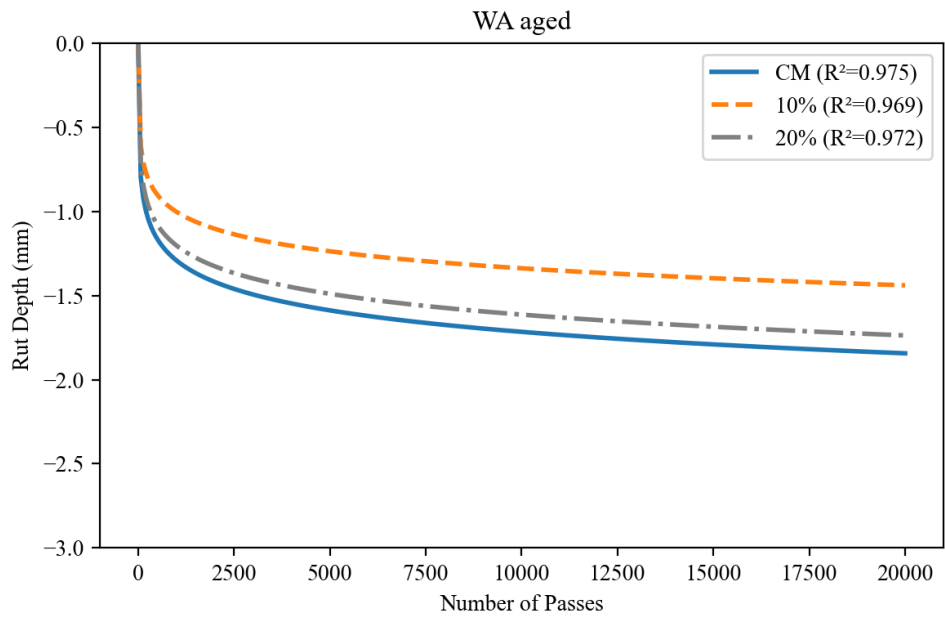


Figure 12. Rut Depth vs No. of Passes for Mixtures at 3 Days of Aging

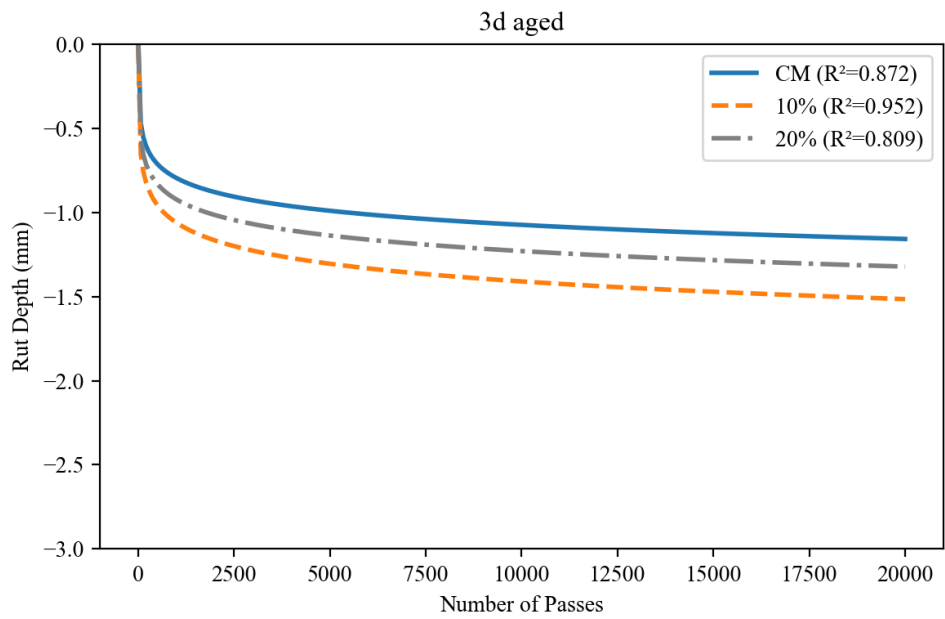


Figure 13. Rut Depth vs No. of Passes for Mixtures at 5 Days of Aging

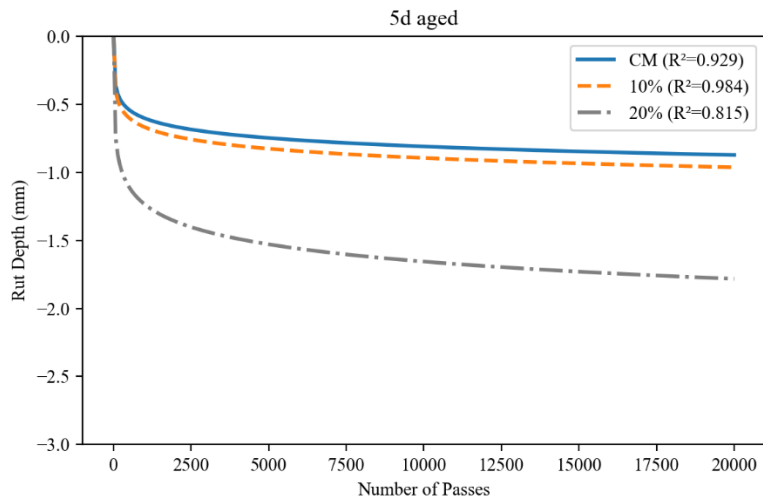


Figure 14. Rut Depth vs No. of Passes for Mixtures at 7 Days of Aging

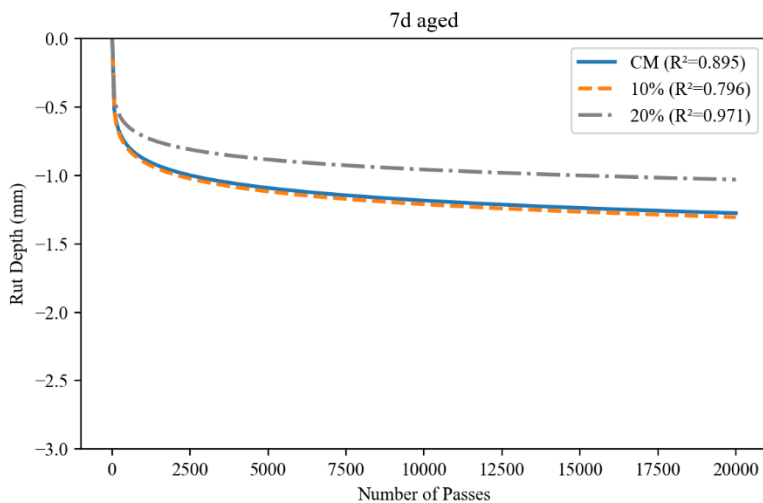
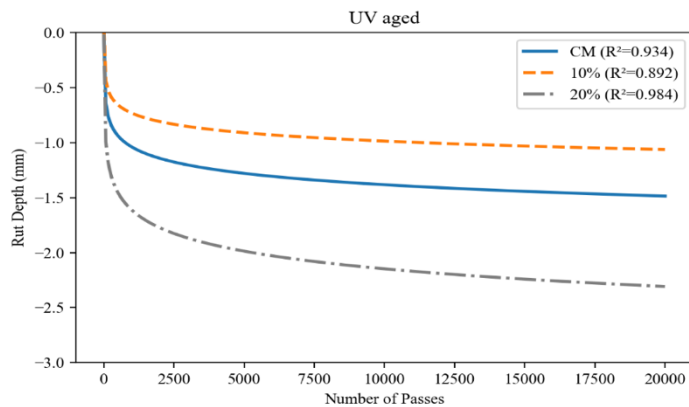


Figure 15. Rut Depth vs No. of Passes for Mixtures at Thermal + UV Aging Level



In determining whether modifier dosage and aging level could affect the rutting performance of asphalt mixtures, a two-factor ANOVA was applied, with rut depth taken as the dependent variable at 15,000 passes. An evaluation of results stated in Table 4 demonstrates that none of the factors under study had a statistically significant impact on the average rut depth. P-values for additive dosage (0%, 10%, 20%) and aging protocol (0 d, 3 d, 5 d, 7 d, UV) were 0.749 and 0.726, respectively, both well above the 0.05 significance threshold. Such findings suggest that the recorded differences in rutting resistance among the mixtures were not attributed to any systemic effect of modifier dosage or aging protocol, but rather were within the realm of experimental variability. Another clear indication of this conclusion is present as well in Table 4, where an extremely low F-value for each factor can be found. This basically means that both modified and unmodified mixtures resisted rutting to the same level, with this confirming that the proposed low-carbon polymeric modifiers can indeed be used as a green alternative without trading off performance.

Table 4. ANOVA Results Rut Depth at 15,000 Passes

Source	DF	Adj SS	Adj MS	F-Value	P-Value
<b>Additive</b> (0%, 10%, 20%)	2	0.380	0.190	0.29	0.749
<b>Aging</b> (0 d / 3 d / 5 d / 7 d / UV)	4	1.333	0.333	0.51	0.726
<b>Error</b>	21	13.602	0.648	—	—
<b>Total</b>	27	15.315	—	—	—

To explore at each aging level whether the modifier has an effect on rutting behavior, a series of one-way ANOVA tests were performed, as summarized in Table 5. The results show that in none of the aging conditions, unaged (0 d), thermally aged (3 d, 5 d, 7 d), or thermally + UV aged (UV), was rutting resistance significantly affected by the additive dosage (0% and 10%). All p-values exceeded the 0.05 threshold, ranging from 0.643 for the unaged specimens, 0.925 (3d), 0.800 (5d), 0.965 (7d), to 0.293 for the UV-aged set, so the null hypothesis could not be rejected at any aging level. The largest F-value was 1.90 for the UV-aged condition; the rest fell between 0.04 and 0.50, confirming the absence of statistically meaningful differences. Note that at the WA level, the 20% dosage group was excluded due to abnormal rutting values, which could disproportionately influence statistical interpretation. Taken together, these findings indicate that incorporating the low-carbon additive system at appropriate dosages does not materially change rutting resistance at 15,000 passes. Consequently, the sustainable modifiers can be adopted without sacrificing early-life rutting performance.

Table 5. One-Way ANOVA of 15000 Pass Rut Depths by Aging Level

Aging	Source	DF	Adj SS	Adj MS	F-Value	P-Value
<b>0d</b>	Factor	1	0.040	0.040	0.5	0.643
	Error	2	1.160	0.080		
	Total	3	0.2			
<b>3d</b>	Factor	2	0.2037	0.1019	0.08	0.925
	Error	3	3.8102	1.2701		
	Total	5	4.014			
<b>5d</b>	Factor	2	0.209	0.1045	0.24	0.8
	Error	3	1.3061	0.4354		
	Total	5	1.5151			
<b>7d</b>	Factor	2	0.0892	0.0446	0.04	0.965
	Error	3	3.6666	1.2222		
	Total	5	3.7558			
<b>UV</b>	Factor	2	1.5745	0.7873	1.9	0.293
	Error	3	1.242	0.414		
	Total	5	2.8165			

Furthermore, the Tukey pair wise test was applied to look for differences between the control and treated mixes at each aging level with respect to rut depths, as shown in Table 6. At the unaged (0d) condition, only the 10% mixture could be compared with the control because the 20% mixture exhibited excessive rutting and its data were removed from the statistical set. Across the remaining aging levels (3d, 5d, 7d, and UV), all three mixtures were included; although small mean differences appeared, for example, the slightly larger separation between 10% and 20% under UV aging, none were statistically significant. All adjusted p-values were above 0.05, and all confidence intervals include zero, implying that these variations are more likely caused by

experimental variability than by intrinsic differences in mixture performance. This outcome thereby supports the broader conclusion that adding low-carbon modifiers at a level of either 10% or 20% does not compromise rutting resistance; in fact, the consistency of the statistical response across aging levels speaks to the robustness of the modified mixtures across both thermal and environmental aging scenarios.

Table 6. Tukey Pair-Wise Comparison Table for Rut Depth at 15,000 Passes

Aging level	Group 1	Group 2	Mean diff (mm)	p_adj	95% CI lower	95% CI upper	Significant? (< 0.05)
0d	10%	CM	0.49	0.82	-2.909	3.889	No
(20%-WA comparisons omitted – see note) *							
3 d	10%	20%	-0.45	0.91	-5.159	4.259	No
	10%	CM	-0.255	0.97	-4.964	4.454	No
	20%	CM	0.195	0.98	-4.514	4.904	No
5 d	10%	20%	0.295	0.89	-2.462	3.052	No
	10%	CM	-0.155	0.97	-2.912	2.602	No
	20%	CM	-0.45	0.78	-3.207	2.307	No
7 d	10%	20%	-0.05	0.99	-4.67	4.57	No
	10%	CM	0.23	0.97	-4.39	4.85	No
	20%	CM	0.28	0.96	-4.34	4.9	No
UV	10%	20%	1.23	0.28	-1.459	3.919	No
	10%	CM	0.4	0.82	-2.289	3.089	No
	20%	CM	-0.83	0.49	-3.519	1.859	No

N/A\*: Values for the 20%-WA mixture are not reported due to the observed significant rut depth after only 6,000 passes. This mix exhibited excessive rutting beyond expected limits, and the data were excluded from analysis to maintain consistency and reliability of the results.

## 7.2 Indirect Tensile Asphalt Cracking Test

The IDEAL-CT test was performed on control and modified asphalt mixtures with 10% and 20% low-carbon additives to assess their resistance to cracking under various aging conditions. The  $CT_{index}$ , which is a key number that comes from this test, tells you how well a mixture can resist cracking from fatigue. In general, higher  $CT_{index}$  values indicate that HMA is less likely to crack. Tables 7 through 11 and Figure 13 show the results for different aging levels: without aging (WA), 3 days, 5 days, 7 days, and thermally + UV-aged. All of the mixtures were fairly resistant to cracking at the without aging level. The mixture with 10% additive content had the highest  $CT_{index}$  (158.6), followed by the 20% mixture (128.4) and the control mix (125.1). These results suggest that adding low-carbon sulfur polymer modifiers made the material more resistant to cracking before it was put under stress from aging. As the mixtures aged for three days, their relative performance changed. The 20% modified mixture had the highest  $CT_{index}$  (97.1), while the 10% mix and control dropped to 59.3 and 40.4, respectively. At this stage, the 20% dosage has a clear advantage, with cracking resistance that is more than 140% better than the control mix.

The control mix showed moderate recovery after 5 days of aging, with a  $CT_{index}$  of 56.7. The 20% modified mix was very close behind, with a value of 50.0. But the 10% mixture dropped a lot to 17.6, which was the lowest CT index seen in any of the conditions. This drop could mean that the 10% dose is temporarily incompatible or sensitive to intermediate thermal oxidation conditions. After 7 days of thermal aging, both modified mixtures worked better than the control. The 20% additive mix had the highest  $CT_{index}$  at 65.3, while the 10% and control mixes had 41.1 and 37.6, respectively. These results indicate that the 20% additive dosage offers improved durability and crack resistance when subjected to prolonged thermal exposure. The performance pattern changed again after UV aging. The 10% modified mixture had the highest  $CT_{index}$  of 70.2, followed by the control at 63.8 and the 20% modified mixture at 51.0. In conclusion, the mixture with 10% modifier shows better resistance to UV-aging compared to the others. Figure 13 clearly demonstrates how the  $CT_{index}$  values for all mixtures change with aging level. As aging levels go higher, cracking resistance gets worse overall, but the relative ranking of how well the mixtures work changes depending on the aging condition. The 20% dose works better during early and middle aging, while the 10% dose works better under UV stress. The control mixture was the least consistent overall.

In summary, the data show that adding things to asphalt mixtures makes them less likely to crack over time. The 20% dosage makes the material more stable when it ages in heat, while the 10% dosage makes it more resistant to UV light. These results show how important it is to choose the right amount of additive based on the most common environmental exposure to make pavement last as long as possible.

Table 7. IDEAL-CT Results for Each Mixture at Without Aging Level

Sample Name	Peak Load (kN)	$I_{75}$ (mm)	$ m_{75} $ (N/m)	$W_f$ (J)	$G_f$ (J/m <sup>2</sup> )	$CT_{index}$
CM-WA-1	14.2	5.1	2759534.8	81.9	8811.1	107.8
CM-WA-2	13.4	5.7	2125312.7	86.2	9263.9	164.5
CM-WA-3	13.0	5.1	2550316.2	71.3	7664.3	103.1
<b>Average</b>	<b>13.5</b>	<b>5.3</b>	<b>2478387.9</b>	<b>79.8</b>	<b>8579.8</b>	<b>125.1</b>
10%-WA-1	7.3	5.2	1300192.6	39.8	4277.9	114.4
10%-WA-2	7.1	6.4	1102154.6	48.2	5183.0	201.6
10%-WA-3	7.3	5.9	1270831.0	48.3	5194.8	159.9
<b>Average</b>	<b>7.2</b>	<b>5.8</b>	<b>1224392.7</b>	<b>45.4</b>	<b>4885.2</b>	<b>158.6</b>
20%-WA-1	5.5	5.4	941756.2	32.9	3541.2	134.7
20%-WA-2	5.4	5.4	886025.1	31.1	3346.8	136.9
20%-WA-3	6.7	5.1	1206797.3	37.6	4044.8	113.6
<b>Average</b>	<b>5.8</b>	<b>5.3</b>	<b>1011526.2</b>	<b>33.9</b>	<b>3644.2</b>	<b>128.4</b>

Table 8. IDEAL-CT Results for Each Mixture at 3 Days of Aging Level

Sample Name	Peak Load (kN)	$I_{75}$ (mm)	$ m_{75} $ (N/m)	$W_f$ (J)	$G_f$ (J/m <sup>2</sup> )	$CT_{index}$
CM-3d-1	14.0	3.6	3963559.7	54.1	5813.2	35.3
CM-3d-2	12.1	4.0	3014167.8	51.5	5533.1	49.3
CM-3d-3	16.9	4.1	5228154.5	64.7	6956.6	36.6
<b>Average</b>	<b>14.3</b>	<b>3.9</b>	<b>4068627.3</b>	<b>56.7</b>	<b>6101.0</b>	<b>40.4</b>
10%-3d-1	12.9	4.1	3056686.6	58.3	6270.6	56.2
10%-3d-2	10.5	4.3	2227829.3	49.0	5272.8	67.2
10%-3d-3	12.9	4.1	3068391.1	56.5	6076.6	54.6
<b>Average</b>	<b>12.1</b>	<b>4.2</b>	<b>2784302.3</b>	<b>54.6</b>	<b>5873.3</b>	<b>59.3</b>
20%-3d-1	11.8	5.0	2309147.1	64.3	6919.1	99.3
20%-3d-2	8.6	4.8	1572573.8	45.9	4938.1	99.9
20%-3d-3	9.7	5.0	2015968.3	51.4	5528.0	92.0
<b>Average</b>	<b>10.0</b>	<b>4.9</b>	<b>1965896.4</b>	<b>53.9</b>	<b>5795.1</b>	<b>97.1</b>

Table 9. IDEAL-CT Results for Each Mixture at 5 Days of Aging Level

Sample Name	Peak Load (kN)	$I_{75}$ (mm)	$ m_{75} $ (N/m)	$W_f$ (J)	$G_f$ (J/m <sup>2</sup> )	$CT_{index}$
CM-5d-1	17.0	3.9	3858935.5	77.4	8323.7	56.7
CM-5d-2	15.4	3.7	4001593.5	60.9	6548.2	40.4
CM-5d-3	15.5	3.0	4820171.0	51.7	5564.4	23.1
<b>Average</b>	<b>17.0</b>	<b>3.9</b>	<b>3858935.5</b>	<b>77.4</b>	<b>8323.7</b>	<b>56.7</b>
10%-5d-1	15.9	3.0	6603243.5	45.1	4851.8	14.8
10%-5d-2	13.7	3.0	5425143.3	41.1	4414.8	16.4
10%-5d-3	12.5	3.4	5433462.4	48.1	5169.9	21.7
<b>Average</b>	<b>14.0</b>	<b>3.2</b>	<b>5820616.4</b>	<b>44.8</b>	<b>4812.2</b>	<b>17.6</b>
20%-5d-1	11.5	4.2	2809953.7	51.6	5550.7	55.7
20%-5d-2	11.8	3.7	3076180.5	47.9	5151.9	41.5
20%-5d-3	13.1	4.5	3401391.6	55.5	5969.2	52.7
<b>Average</b>	<b>12.1</b>	<b>4.2</b>	<b>3095841.9</b>	<b>51.7</b>	<b>5557.3</b>	<b>50.0</b>

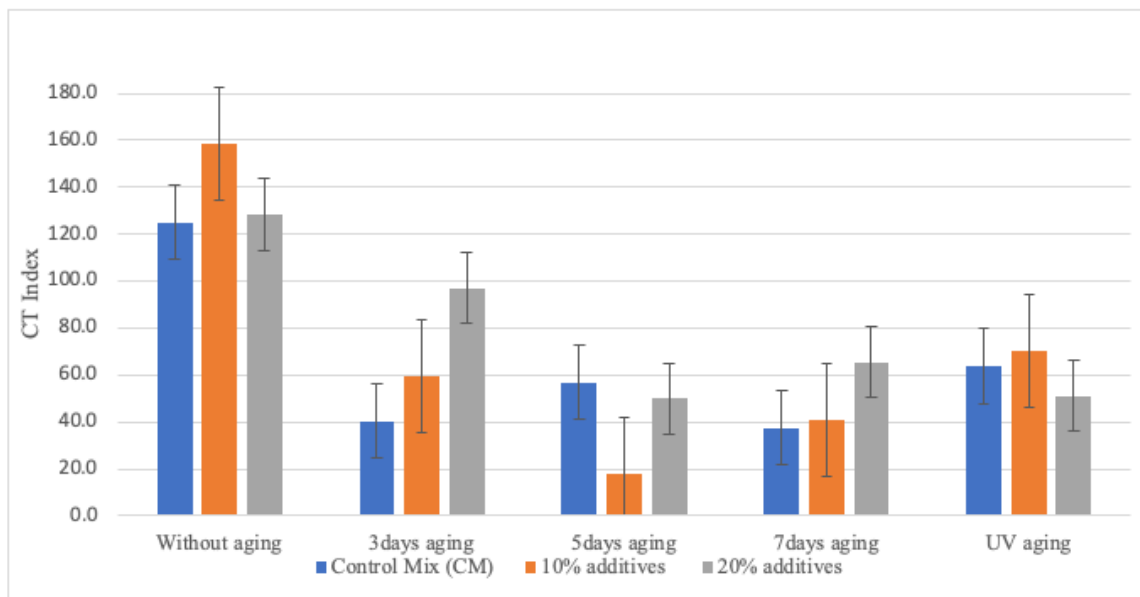
Table 10. IDEAL-CT Results for Each Mixture at 7 Days of Aging Level

Sample Name	Peak Load (kN)	$I_{75}$ (mm)	$ m_{75} $ (N/m)	$W_f$ (J)	$G_f$ (J/m <sup>2</sup> )	$CT_{index}$
CM-7d-1	15.0	3.8	4017034.3	62.9	6759.7	42.3
CM-7d-2	16.0	5.1	6360360.6	72.2	7766.2	41.3
CM-7d-3	16.9	3.3	4858811.6	60.4	6492.4	29.2
<b>Average</b>	<b>15.9</b>	<b>4.0</b>	<b>5078735.5</b>	<b>65.2</b>	<b>7006.1</b>	<b>37.6</b>
10%-7d-1	16.9	3.5	5228928.2	62.9	6761.9	30.0
10%-7d-2	13.4	4.1	3352053.8	57.8	6212.8	50.8
10%-7d-3	16.0	4.6	4934997.3	63.6	6834.6	42.7
<b>Average</b>	<b>15.4</b>	<b>4.1</b>	<b>4505326.4</b>	<b>61.4</b>	<b>6603.1</b>	<b>41.1</b>
20%-7d-1	10.7	4.5	2553887.4	49.3	5300.8	62.1
20%-7d-2	11.2	4.5	2518172.3	53.9	5794.9	68.5
20%-7d-3	13.4	3.8	3652775.7	52.6	5659.6	39.2
<b>Average</b>	<b>10.9</b>	<b>4.5</b>	<b>2536029.9</b>	<b>51.6</b>	<b>5547.9</b>	<b>65.3</b>

Table 11. IDEAL-CT Results for Each Mixture at Thermal + UV Aging Level

Sample Name	Peak Load (kN)	$I_{75}$ (mm)	$ m_{75} $ (N/m)	$W_f$ (J)	$G_f$ (J/m <sup>2</sup> )	$CT_{index}$
CM-UV-1	16.8	4.6	3973629.9	78.1	8399.5	64.8
CM-UV-2	14.8	4.9	3468345.6	69.2	7443.2	70.5
CM-UV-3	17.6	4.7	4556886.7	76.2	8197.5	56.0
<b>Average</b>	<b>16.4</b>	<b>4.7</b>	<b>3999620.7</b>	<b>74.5</b>	<b>8013.4</b>	<b>63.8</b>
10%-UV-1	12.5	4.6	2440740.3	62.6	6731.6	84.9
10%-UV-2	11.6	4.4	2448920.6	55.1	5926.3	70.4
10%-UV-3	13.8	4.8	3663470.9	59.4	6382.4	55.3
<b>Average</b>	<b>12.6</b>	<b>4.6</b>	<b>2851043.9</b>	<b>59.0</b>	<b>6346.7</b>	<b>70.2</b>
20%-UV-1	12.2	3.9	3092741.7	51.7	5555.5	47.1
20%-UV-2	13.8	4.0	3817752.2	57.6	6192.6	42.9
20%-UV-3	10.1	4.4	2601707.8	51.4	5531.5	63.0
<b>Average</b>	<b>12.0</b>	<b>4.1</b>	<b>3170733.9</b>	<b>53.6</b>	<b>5759.8</b>	<b>51.0</b>

Figure 16.  $CT_{index}$  for Mixtures



Figures 17 to 21 show the load versus deformation curves for the control mix (CM), 10% modifier, and 20% modifier asphalt mixtures under five different aging conditions: without aging (WA), 3 days, 5 days, 7 days, and thermal plus UV aging. These curves show the average behavior of the replicates, allowing you to compare the post-peak slope characteristics that indicate the brittleness or ductility of each mix. When the CM mixture was not aged (Figure 17), it had the highest peak load, followed by the 10% and 20% additive mixtures. The CM curve showed a clear drop after the peak, which means that the strength dropped sharply after cracking. The additive mixtures, on the other hand, had flatter slopes, especially at 20%, which means that they were more ductile after cracking. This fits with the idea that modifiers make the mix softer at first, which makes it more flexible early on. In Figure 18, which shows 3-day aging, all of the curves moved up in terms of peak load. This is because the binder stiffened as it oxidized. However, the behavior after the peak was different: The CM mix had a steep slope, indicating it was likely to fail in a brittle manner. The 20% additive mix, on the other hand, had a lower peak load but a flatter post-peak slope and a longer deformation capacity. This shows that ductility was still present even after the material had aged. The 10% mix, on the other hand, had intermediate peak and slope values, which suggests that the failure mode was changing.

Five-day aging (Figure 19) maintained the CM curve's steepness up to the highest peak; in contrast, both additive mixtures showed diminished peak loads and narrower deformation ranges. This implies over-stiffening at 10%, wherein aging tends to help the mix into a fragile regime, and with no room for adjustment in the form of flexibility, the 10% mix was found to exhibit one of the lowest  $CT_{index}$ . The mixture at 20% is stiffer, but it still showed a wider deformation tail and hence, an intermediate tolerance to cracks.

The 7-day aging curves, as shown in Figure 20, exhibited an explicit pattern: The peak loads of these mixtures were the same, but the post-peak falloff of 10% was more gradual than that of CM and 20%. The CM mixture presented sharp strength losses after peaks, while in the case of the 20% additive mix, the strength loss was more uniform, thus realizing a better trade-off between peak capacity and deformation. This may imply that the modified mixes have better energy dissipation properties with further aging.

Lastly, the UV-aged condition (Figure 21) presents a clear picture of the drop in deformation capacity in all mixtures among noticeable differences in peak loads; the CM mix had the highest load with the steepest drop post-peak, characteristic of brittle fracture. The additive mixes, mainly 10%, maintained flatter post-peak slopes and greater deformation spans, making them more fracture-resistant during environmental aging.

Collectively, these load-deformation trends reinforce the  $CT_{index}$  results and show key mechanical distinctions. A CM mix tends to become more brittle with aging, while additive-modified mixes, improved at 10%, demonstrate a more balanced behavior depending on aging

severity. At the same time, the 20% mix tends to show improved ductility but at the expense of strength; hence, the tradeoff between the two is stiffness versus cracking resistance. These patterns suggest that the optimized level of additive dosage must be regarded as the key parameter for engineering mechanical behavior across the pavement's service life.

Figure 17. Load vs Deformation Curves for Mixtures at Without Aging Level

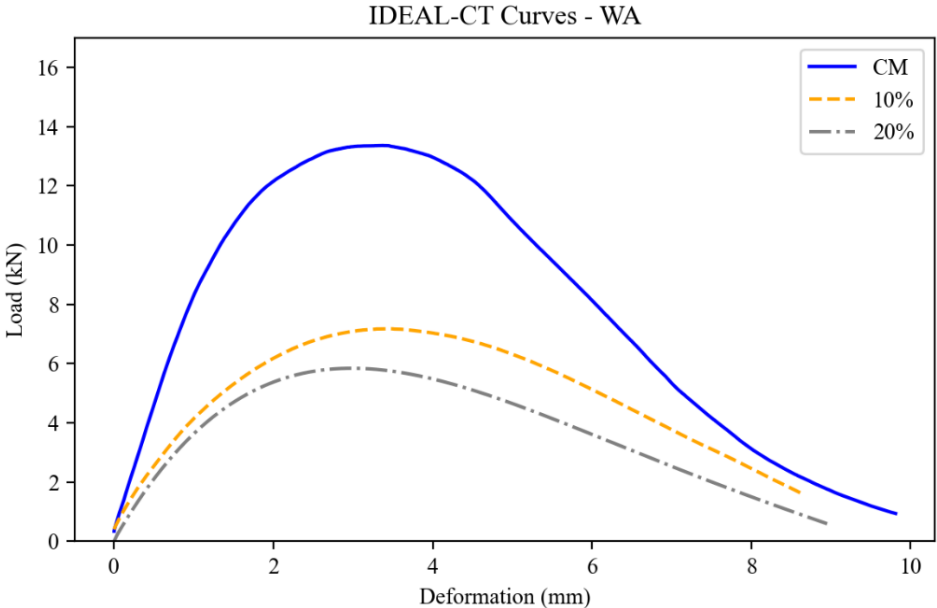


Figure 18. Load vs Deformation Curves for Mixtures at 3 Days of Aging Level

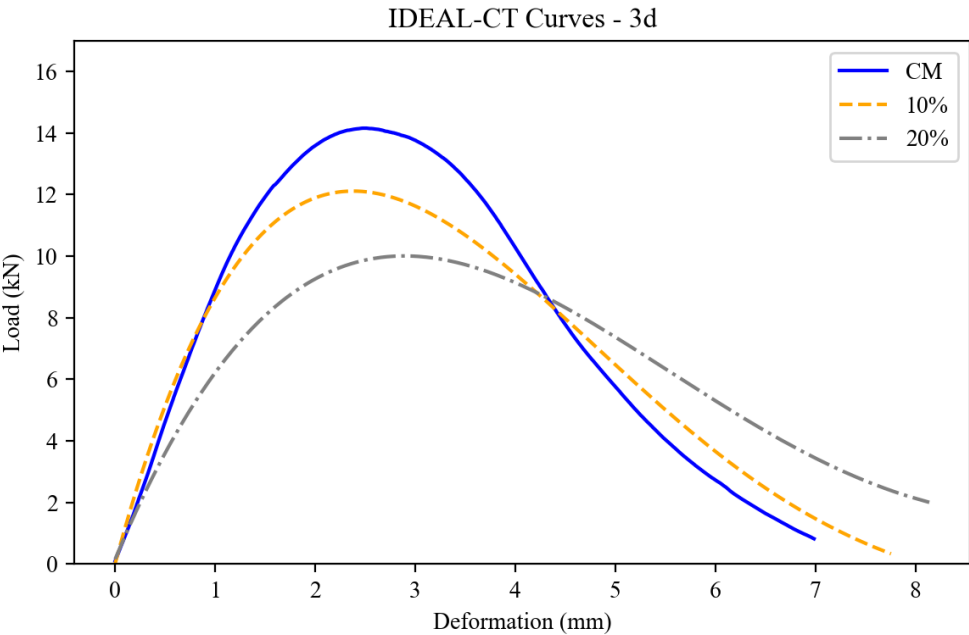


Figure 19. Load vs Deformation Curves for Mixtures at 5 Days of Aging Level

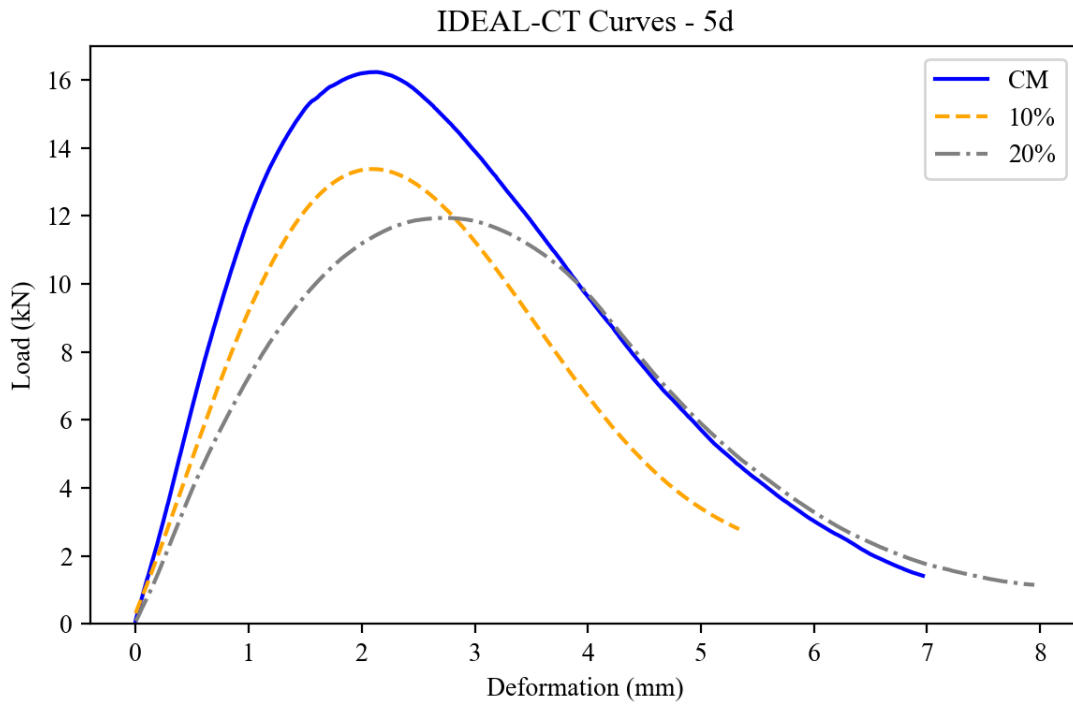


Figure 20. Load vs Deformation Curves for Mixtures at 7 Days of Aging Level

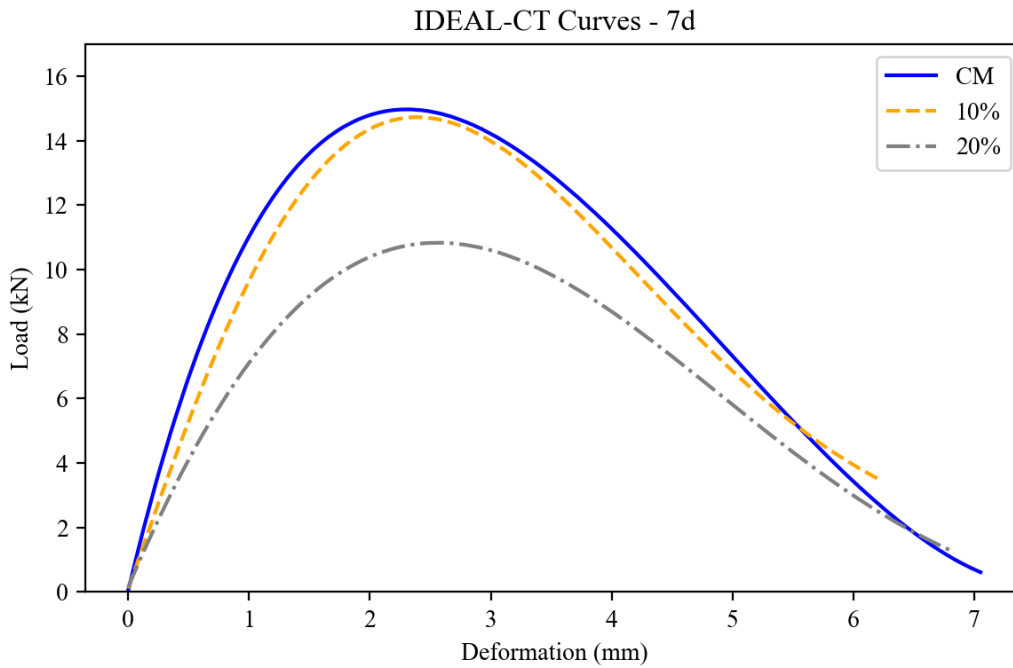


Figure 21. Load vs Deformation Curves for Mixtures at Thermal + UV Aging Level

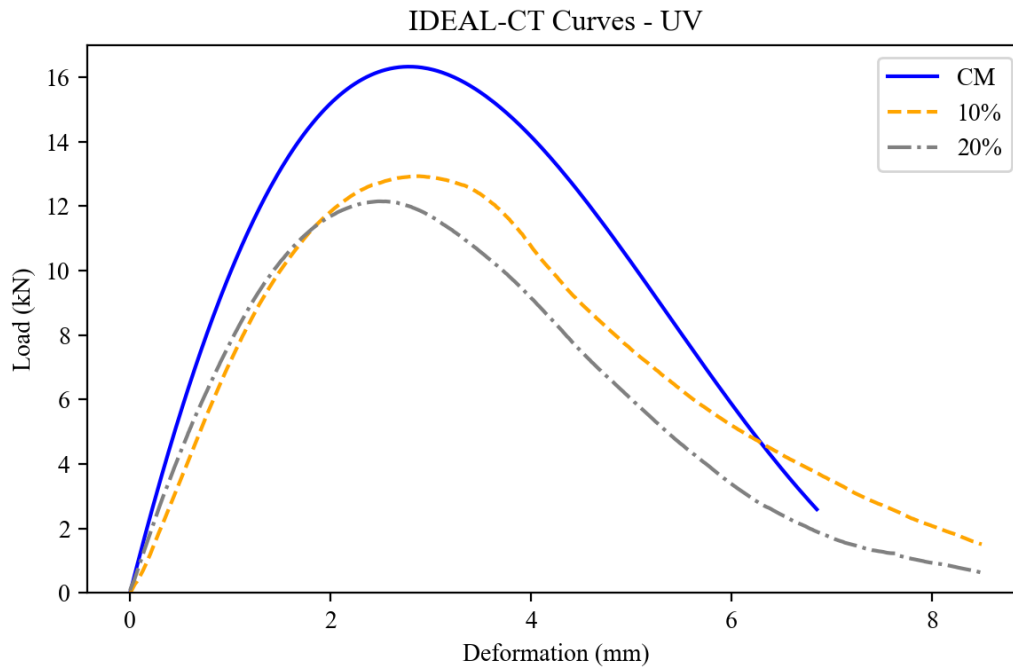
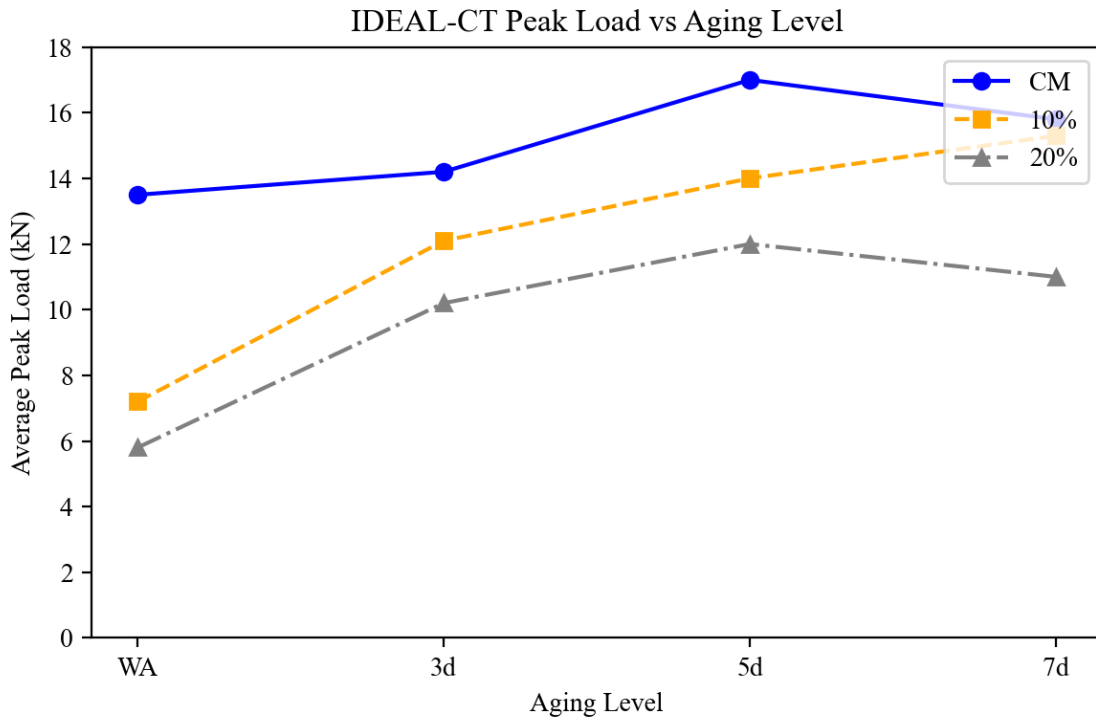


Figure 19 shows the peak load values for each mixture versus level of aging. Peak load, which is the highest load that can be sustained before a fracture starts, usually increases as the mixtures age. This result is due to the binder oxidizing, which leads to a stiffer mixture. The control mix (CM) had the highest peak load at all aging levels, with the highest load at 5 days and the lowest load at 7 days. The 10% modified mixture showed a steady rise in peak load over the course of 7 days, which suggests that it is more stable when exposed to heat. On the other hand, the 20% mixture showed a similar trend for the first five days, but the peak load dropped significantly on the seventh day, which could indicate that embrittlement is starting to happen. A look at these peak load trends along with the  $CT_{index}$  and post-peak deformation characteristics, indicates how stiffness gain and cracking tolerance work together in aging asphalt mixtures. These observations indicate that although elevated peak load signifies enhanced stiffness, it does not inherently imply improved cracking resistance. The 10% additive appears to make the mechanical response more balanced by introducing some stiffness without compromising ductility. The 20% additive, on the other hand, could make the mixtures too stiff and cause them to break easily when they get older.

Figure 22. Peak Load vs Level of Aging



Independent two-sample t-tests were performed on the  $CT_{index}$  values at each aging level to determine the statistical significance of differences in cracking resistance among mixtures. Table 12 shows the p-values for all pair wise comparisons between the control mix (CM), the 10% additive mixture, and the 20% additive mixture. The significance level was set at  $\alpha = 0.05$ .

For mixtures without aging, none of the comparisons showed statistically significant differences in  $CT_{index}$ , which means that all three mixtures had the same amount of cracking resistance before aging. However, at the 3-day aging level, all pair wise comparisons showed some differences. The  $CT_{index}$  of the 10% mixture was significantly greater than that of the 20% mixture ( $p = 0.0013$ ), and both modified mixtures exhibited significant differences from the control ( $p = 0.0338$  and  $p = 0.0004$  for CM vs 10% and CM vs 20%, respectively). These results indicate that the effect of additive content intensifies following initial aging. At the 5-day aging level, the only statistically significant difference was between the 10% and 20% mixtures ( $p = 0.0044$ ). There was no significant difference between either modified and control mixtures. This could mean that the  $CT_{index}$  for the 10% mix, dropped more quickly between days 3 and 5 than the 20% mix, which would explain the smaller performance gap seen earlier.

There were no significant differences between any of the mixtures at the 7-day and UV aging levels. The convergence of  $CT_{index}$  values at these advanced aging stages indicates that the

prolonged oxidative effects ultimately diminish the unique contributions made by the modifiers, leading to comparable cracking performance irrespective of additive content.

In general, the t-test results demonstrate the importance of evaluating a mixture's effectiveness at various stages of aging. The 10% additive level does better than others at first when the aging conditions are moderate, but its relative advantage fades over time. This shows how complicated the relationship is between additive dosage and long-term durability.

Table 12. T-Test for Pair wise  $CT_{index}$  Comparisons at Each Aging Level

Aging level	Comparison	p-value	Significant? (< 0.05)
without aging	CM vs 10%	0.3541	No
	CM vs 20%	0.8844	No
	10% vs 20%	0.3136	No
3 d	CM vs 10%	0.0338	Yes
	CM vs 20%	0.0004	Yes
	10% vs 20%	0.0013	Yes
5 d	CM vs 10%	0.0866	No
	CM vs 20%	0.3303	No
	10% vs 20%	0.0044	Yes
7 d	CM vs 10%	0.6539	No
	CM vs 20%	0.1257	No
	10% vs 20%	0.2247	No
UV	CM vs 10%	0.5366	No
	CM vs 20%	0.1610	No
	10% vs 20%	0.1418	No

To examine the statistical significance of  $CT_{index}$  in greater depth, Tukey's Honest Significant Difference (HSD) test is used to investigate the differences between mixtures at each aging stage. The results are shown in Table 13. This post-hoc analysis enhances the previously examined t-test results by accounting for multiple comparisons and offering confidence intervals for the mean differences. When there was no aging, none of the comparisons were statistically significant ( $p\text{-adj} > 0.05$ ), and the confidence intervals for all group comparisons included zero. This means that, before any aging, all mixtures, despite the amount of modifier they had, had statistically similar cracking resistance. There were clear differences at the 3-day aging level. All three pair wise comparisons were statistically significant ( $p\text{-adj} < 0.05$ ). The 10% modified mixture

had a  $CT_{index}$  that was significantly higher than the 20% mixture and significantly lower than the control. The most noticeable difference was between the control and 20%, which suggests that the 20% dosage may have made the material less resistant to cracking as it aged. At the 5-day aging level, the only statistically significant difference was seen between the 10% and 20% mixtures ( $p\text{-adj} = 0.02$ ). This shows that the two additive levels are still performing differently. However, the differences between each modified mixture and the control were not statistically significant, indicating a degree of convergence in  $CT_{index}$  values at this aging point. As aging progressed to 7 days and UV exposure, no statistically significant differences were observed among any group combinations. The  $p\text{-adj}$  values in these comparisons were higher than 0.05, and the confidence intervals included zero, which means that the performance ranges were the same. This result suggests that the long-term consequences of oxidative and UV aging tend to reduce the statistical distinctiveness among mixes, possibly due to the saturation of aging effects or the homogenization of stiffness and fracture behavior. To sum up, the Tukey HSD results show that the amount of additive has a big effect on  $CT_{index}$  performance when the material is moderately aged (especially after 3 days), but this effect gets weaker as the material ages more. These results support the idea that performance benefits are only temporary and show how important it is to do long-term durability tests when looking at improvements to asphalt mixtures.

Table 13. Tukey HSD Pair-Wise Comparisons of  $CT_{index}$  Aging Level

Aging level	Comparison	Mean diff	p-adj	95% CI lower	95% CI upper	Significant? (< 0.05)
without aging	10% vs 20%	-30.23	0.53	-112.51	52.04	No
	10% vs CM	-33.5	0.47	-115.77	48.77	No
	20% vs CM	-3.27	0.99	-85.54	79.01	No
3 d	10% vs 20%	37.73	0.00	21.48	53.98	Yes
	10% vs CM	-18.93	0.03	-35.18	-2.68	Yes
	20% vs CM	-56.67	0.00	-72.92	-40.42	Yes
5 d	10% vs 20%	34.87	0.02	6.25	63.48	Yes
	10% vs CM	22.43	0.12	-6.18	51.05	No
	20% vs CM	-12.43	0.43	-41.05	16.18	No
7 d	10% vs 20%	15.43	0.30	-13.51	44.38	No
	10% vs CM	-3.57	0.93	-32.51	25.38	No
	20% vs CM	-19	0.19	-47.94	9.94	No
UV	10% vs 20%	-19.2	0.18	-47.57	9.17	No
	10% vs CM	-6.43	0.77	-34.81	21.94	No
	20% vs CM	12.77	0.41	-15.61	41.14	No

Table 14. Summary of Test Results by Level of Aging

	$CT_{index}$			HWT		
	CM	10%	20%	CM	10%	20%
Without Aging	125.1	158.6	128.4	-1.74	-1.26	N/A
3 Days	40.4	59.3	97.1	-1.36	-1.61	-1.16
5 Days	56.7	17.6	50	-0.8	-0.96	-1.25
7 Days	37.6	41.1	65.3	-1.36	-1.12	-1.08
UV	63.8	70.2	51	-1.42	-1.15	-2.27

Table 15. Summary of Tukey Pair wise Comparison for All Tests

Test Type	Comparison	Without Aging	3 Days	5 Days	7 Days	UV Aging
Rut Depth	10% vs 20%	NS	NS	S	NS	NS
	10% vs CM	N/A	NS	NS	NS	NS
	20% vs CM	N/A	NS	NS	NS	NS
<b>CT<sub>index</sub></b>	10% vs 20%	NS	S	S	NS	NS
	10% vs CM	NS	S	NS	NS	NS
	20% vs CM	NS	S	NS	NS	NS

## 8. Summary and Conclusions

### 8.1. Conclusions

This study assessed the efficacy of asphalt mixtures enhanced with a low-carbon additive system, consisting of elemental sulfur, biochar, and waste cooking oil (WCO) at 10% and 20% dosages, in comparison to a conventional control mix. To simulate the oxidative and environmental stresses that happen in the field, the mixtures were tested under a range of short- and long-term aging conditions, including without aging; 3, 5, 7 days of ageing; and a combination of thermal and UV aging. The IDEAL-CT test (for cracking resistance) and the Hamburg Wheel Tracking test (for rutting resistance) were used to measure mechanical properties.

The findings indicated that aging uniformly resulted in diminished cracking resistance across all mixtures, as evidenced by declining  $CT_{index}$  values. After aging, the CM mix showed a big drop in crack resistance. The 10% modified mixture showed better UV aging resistance and better cracking performance when it was not aged and when it was aged for three days. However, it dropped significantly at the five-day aging stage. The 20% modified mixture worked better after 3, 5, and 7 days of aging, but it did not hold up as well when it was UV-aged.

With the exception of the unaged 20% mixture, which exhibited excessive rut depth and was excluded from the statistical analysis, all mixtures remained below 3 mm after 15,000 passes, indicating satisfactory rutting resistance under the accepted Caltrans criterion. The 20% mixture showed the smallest rut depth under the combined thermal + UV protocol (despite its poor unaged rutting response), suggesting potential for applications where severe oxidative environments dominate the pavement's service life. However, such contrasted behavior of the 20% dosage, good rutting resistance after aging but poor rutting in the unaged stage, highlights a dosage-dependent trade-off between early-life deformability and long-term stiffness.

Using t-tests and Tukey HSD, statistical analyses found that there were only significant differences in  $CT_{index}$  at the beginning of the aging process, especially after 3 days, and mostly between the control and 10% or 20% mixes. As time went on, though, the statistical significance went down, which meant that the long-term performance of the mixtures was more similar.

The load-deformation curves confirmed these results, showing that the 10% mix usually had a flatter slope after the peak, which means it was more ductile when loaded. The 20% mix, on the other hand, often had higher peak loads but also had stiffer and sometimes more brittle responses, depending on how long it had been aging.

The summary of the final results showed that no one mixture did better than the others on all performance metrics. Instead, each one had benefits when it was aged in certain ways. On balance, the 10% dosage offers the most consistent compromise between cracking and rutting resistance across all aging scenarios. The 20% dosage provides superior rutting resistance once the pavement has been thermally or UV-aged, but its excessive deformation in the unaged state suggests that further formulation or construction adjustments (e.g., higher compaction, stiffer base) would be required before field deployment.

In general, adding a low-carbon additive system made up of WCO, elemental sulfur, and biochar to asphalt pavements looks like it could make them more durable and environmentally friendly. These results suggest that more research should be done on finding the best dosages and how well binders and additives work together, especially in places where oxidative aging and rutting are big problems. The study underscores the necessity of assessing both the aging stage and the additive composition in the design of asphalt mixtures for enduring performance.

## **8.2 Limitations and Recommendations**

### **8.2.1 Limitations of the Study**

While this study provides valuable insight into the performance of ternary-modified high-RAP asphalt mixtures under thermal and UV aging, several limitations should be acknowledged:

- **Limited Field Validation**

All experimental results were obtained from laboratory-scale testing. Although long-term oven aging and UV protocols were selected to simulate real-world conditions based on NCHRP 973, actual field performance may vary due to additional factors such as traffic loads, environmental fluctuations, and construction variability.

- **Fixed Additive Dosages**

The study evaluated only two dosage levels (10% and 20%) of the sulfur–WCO–biochar blend. Intermediate or lower dosages were not examined, and the optimal content for balancing rutting and cracking resistance may lie outside the tested range.

- **Absence of Binder-Level Chemical Analysis**

While mixture performance was assessed using mechanical tests (IDEAL-CT, HWT), no spectroscopic or chemical characterization (e.g., FTIR, DSR on recovered binder) was conducted to quantify aging resistance mechanisms or additive interactions at the binder scale.

- **No Moisture Sensitivity Testing under Repeated Conditioning**

The moisture susceptibility evaluation was limited to dry conditioning and controlled lab environments. The lack of repeated freeze–thaw cycles or long-term water saturation testing may underestimate moisture-related degradation, especially under field conditions.

- Static Environmental Parameters

UV intensity, oven temperature, and humidity levels were held constant during aging. However, in-field UV radiation and thermal exposure fluctuate diurnally and seasonally, which may influence long-term behavior differently than controlled lab conditions.

### 8.2.2 Recommendations for Future Work

To build upon the findings of this study and further support the implementation of sustainable asphalt technologies, several directions for future research are recommended. First, the laboratory findings should be validated through field trials or Accelerated Pavement Testing (APT) to capture real-time mechanical and environmental effects, including traffic-induced loading and moisture infiltration. Expanding the dosage range of the additive system is also recommended. Future studies should investigate additional additive contents (e.g., 15%) and examine the effects of adjusting the proportions of individual components within the ternary blend to identify the most cost-effective and performance-balanced mixture design.

Further research should include binder recovery from aged mixtures followed by rheological and spectroscopic analyses, such as complex modulus ( $G^*$ ), phase angle ( $\delta$ ), and carbonyl index measurements, to provide deeper insight into the aging mechanisms and interactions within the sulfur–WCO–biochar system. In addition, long-term moisture damage and freeze–thaw resistance should be evaluated using protocols such as AASHTO T 283 (TSR with conditioning) or modified Lottman tests to better quantify moisture-induced deterioration under more aggressive environmental conditions.

Finally, life-cycle cost analysis (LCCA) and life-cycle assessment (LCA) should be conducted to evaluate the economic feasibility and environmental benefits of the ternary-modified mixtures relative to conventional asphalt mixtures. Future work should also investigate the influence of aggregate gradation on mixture performance to optimize structural integrity and compatibility with the ternary binder system. Adjusting the aggregate gradation may improve load distribution, reduce air voids, and enhance both rutting and cracking resistance. In addition, exploring the use of stiffer binder grades, such as PG 64-22 or PG 70-22, in combination with the low-carbon additive system may further improve rutting resistance, particularly in high-temperature climates.

## Bibliography

- AASHTO T 166-22. (2022a). Standard method of test for bulk specific gravity (Gmb) of compacted asphalt mixtures using saturated surface-dry specimens.
- AASHTO T 324-22. (2022b). Standard method of test for Hamburg Wheel-Track Testing of compacted asphalt mixtures.
- AASHTO T 209-22. (2022c). Standard method of test for theoretical maximum specific gravity (Gmm) and density of asphalt mixtures.
- AASHTO R 30-22. (2022d). Standard practice for laboratory conditioning of asphalt mixtures.
- Abdelsalam, M., Yue, Y., Khater, A., Luo, D., Musanyufu, J., and Qin, X. (2020). Laboratory study on the performance of asphalt mixes modified with a novel composite of diatomite powder and lignin fiber. *Applied Sciences (Switzerland)*, 10(16).  
<https://doi.org/10.3390/app10165517>
- Bi, Y., Xu, Y., Li, B., Zou, X., Gao, J., and Li, Q. (2024). Laboratory-accelerated simulation and calibration method for ultraviolet aging of asphalt binders based on radiation equivalent conversion. *Construction and Building Materials*, 435.  
<https://doi.org/10.1016/j.conbuildmat.2024.136791>
- Bilema, M., Aman, M. Y., Hassan, N. A., Al-Saffar, Z., Mashaan, N. S., Memon, Z. A., Milad, A., and Yusoff, N. I. M. (2021). Effects of waste frying oil and crumb rubber on the characteristics of a reclaimed asphalt pavement binder. *Materials*, 14(13).  
<https://doi.org/10.3390/ma14133482>
- Coleri, E., Zhang, Y., and Wruck, B. M. (2018). Mechanistic-Empirical simulations and life-cycle cost analysis to determine the cost and performance effectiveness of asphalt mixtures containing recycled materials. *Transportation Research Record*, 2672(40), 143–154.  
<https://doi.org/10.1177/0361198118776479>
- Filho, W. U., Gutiérrez Klinsky, L. M., Motta, R., & Bernucci, L. L. B. (2020). Cold recycled asphalt mixture using 100% RAP with emulsified asphalt-recycling agent as a new pavement base course. *Advances in Materials Science and Engineering*, 2020, Article 5863458, 1–11. <https://doi.org/10.1155/2020/5863458>
- Hung, A., and Fini, E. H. (2020). Surface morphology and chemical mapping of UV-aged thin films of bitumen. *ACS Sustainable Chemistry and Engineering*, 8(31), 11764–11771.  
<https://doi.org/10.1021/acssuschemeng.0c03877>

- Kar, S. S., Swamy, A. K., Tiwari, D., and Jain, P. K. (2018). Impact of recycled asphalt pavement on properties of foamed bituminous mixtures. *Baltic Journal of Road and Bridge Engineering*, 13(1), 14–22. <https://doi.org/10.3846/bjrbe.2018.383>
- Kim, Y. R., Castorena, C., Elwardany, M., Rad, Y., Underwood, S., Gundha, A., Gudipudi, P., Farrar, M. J., and Glaser, R. R. (2021). Long-term aging of asphalt mixtures for performance testing and prediction: Phase III results. <https://doi.org/10.17226/26133>
- Li, L., Guo, Z., Ran, L., and Zhang, J. (2020). Study on low-temperature cracking performance of asphalt under heat and light together conditions. *Materials*, 13(7). <https://doi.org/10.3390/ma13071541>
- Li, S., Fan, M., Xu, L., Tian, W., Yu, H., and Xu, K. (2021). Rutting performance of semi-rigid base pavement in RIOHTrack and laboratory evaluation. *Frontiers in Materials*, 7. <https://doi.org/10.3389/fmats.2020.590604>
- Lima, M. S. S., Hajibabaei, M., Hesarkazzazi, S., Sitzenfrei, R., Buttgerit, A., Queiroz, C., Tautschnig, A., and Gschösser, F. (2020). Environmental potentials of asphalt materials applied to urban roads: Case study of the city of Münster. *Sustainability (Switzerland)*, 12(15). <https://doi.org/10.3390/su12156113>
- Liu, H., Zhang, Z., Tian, Z., and Lu, C. (2022). Exploration for UV aging characteristics of asphalt binders based on response surface methodology: Insights from the UV aging influencing factors and their interactions. *Construction and Building Materials*, 347. <https://doi.org/10.1016/j.conbuildmat.2022.128460>
- Luo, Y., and Zhang, K. (2023). Review on performance of asphalt and asphalt mixture with waste cooking oil. *Materials*, 16(4). <https://doi.org/10.3390/ma16041341>
- Lyu, L., Pei, J., Burnham, N. A., Fini, E. H., and Poulikakos, L. D. (2023). Nanoscale evolution of rubber-oil modified asphalt binder after thermal and UV aging. *Journal of Cleaner Production*, 426. <https://doi.org/10.1016/j.jclepro.2023.139098>
- Lyu, L., Pei, J., Hu, D., and Fini, E. H. (2021). Durability of rubberized asphalt binders containing waste cooking oil under thermal and ultraviolet aging. *Construction and Building Materials*, 299. <https://doi.org/10.1016/j.conbuildmat.2021.124282>
- Majidifard, H., Tabatabaee, N., and Buttlar, W. (2019). Investigating short-term and long-term binder performance of high-RAP mixtures containing waste cooking oil. *Journal of Traffic and Transportation Engineering (English Edition)*, 6(4), 396–406. <https://doi.org/10.1016/j.jtte.2018.11.002>

- Mousavi, M., Zhou, T., Dong, Z., and Fini, E. H. (2023). Turning abundant waste sulfur to polymers for manufacturing: Exploiting role of organic crosslinkers and benign catalysts. *Journal of Industrial and Engineering Chemistry*, *117*, 205–212. <https://doi.org/10.1016/j.jiec.2022.10.005>
- Mousavi, M., Zhou, T., Liu, R., Dong, Z., and Fini, E. H. (2024). Advancing sustainability with inverse vulcanization of waste sulfur catalyzed with TiO<sub>2</sub>. *Journal of Environmental Chemical Engineering*, *12*(1). <https://doi.org/10.1016/j.jece.2023.111687>
- O’Rear, E. A., Dugan, C. R., Sumter, C. R., Rani, S., Ali, S. A., and Zaman, M. (2020). Rheology of virgin asphalt binder combined with high percentages of RAP binder rejuvenated with waste vegetable oil. *ACS Omega*, *5*(26), 15791–15798. <https://doi.org/10.1021/acsomega.0c00377>
- Pahlavan, F., Aldagari, S., Park, K. B., Kim, J. S., and Fini, E. H. (2023). Bio-Carbon as a means of carbon management in roads. *Advanced Sustainable Systems*, *7*(6). <https://doi.org/10.1002/adsu.202300054>
- Park, K.-B., Chae, D.-Y., Fini, E. H., and Kim, J.-S. (2024). Pyrolysis of biomass harvested from heavy-metal contaminated area: Characteristics of bio-oils and biochars from batch-wise one-stage and continuous two-stage pyrolysis. *Chemosphere*, *355*, 141715. <https://doi.org/10.1016/j.chemosphere.2024.141715>
- Rajib, A., and Fini, E. H. (2020). Inherently functionalized carbon from lipid and protein-rich biomass to reduce ultraviolet-induced damages in bituminous materials. *ACS Omega*, *5*(39), 25273–25280. <https://doi.org/10.1021/acsomega.0c03514>
- Rajib, A., Saadeh, S., Katawal, P., Mobasher, B., and Fini, E. H. (2021). Enhancing biomass value chain by utilizing biochar as a free radical scavenger to delay ultraviolet aging of bituminous composites used in outdoor construction. *Resources, Conservation and Recycling*, *168*. <https://doi.org/10.1016/j.resconrec.2020.105302>
- Rondón-Quintana, H. A., Reyes-Lizcano, F. A., Chaves-Pabón, S. B., Bastidas-Martínez, J. G., and Zafra-Mejía, C. A. (2022). Use of biochar in asphalts: Review. *Sustainability (Switzerland)*, *14*(8). <https://doi.org/10.3390/su14084745>
- Saadeh, S., Al-Zubi, Y., Katawal, P., Zaatarah, B., and Fini, E. (2023). Biochar effects on the performance of conventional and rubberized HMA. *Road Materials and Pavement Design*, *24*(1), 156–172. <https://doi.org/10.1080/14680629.2021.2012238>
- Saadeh, S., and Katawal, P. (2022). Evaluation of Polymer Binder Technisoil G5® in concrete mixture. *Mineta Transport Institute*. <https://doi.org/10.31979/mti.2022.2139>

- Sedthayutthaphong, N., Jitsangiam, P., Nikraz, H., Pra-Ai, S., Tantanee, S., and Nusit, K. (2021). The influence of a field-aged asphalt binder and aggregates on the skid resistance of recycled hot mix asphalt. *Sustainability* (Switzerland), *13*(19).  
<https://doi.org/10.3390/su131910938>
- Wang, X., Fan, Z., Li, Wang, H., and Huang, M. (2019). Durability evaluation study for crumb rubber-asphalt pavement. *Applied Sciences* (Switzerland), *9*(16).  
<https://doi.org/10.3390/app9163434>
- Wei, M., Wu, S., Zhu, L., Li, N., and Yang, C. (2021). Environmental impact on VOCs emission of a recycled asphalt mixture with a high percentage of rap. *Materials*, *14*(4), 1–16.  
<https://doi.org/10.3390/ma14040947>
- Yang, L., Xi, D., Jianzhong, P., Rui, L., Jiupeng, Z., and Tao, L. (2020). Investigation on preparation and rheological properties of grafted organic long-chain carbonitride (CNDC) modified asphalt. *Construction and Building Materials*, *262*.  
<https://doi.org/10.1016/j.conbuildmat.2020.120539>
- Yaro, N. S. A., Sutanto, M. H., Habib, N. Z., Usman, A., Kaura, J. M., Murana, A. A., Birniwa, A. H., and Jagaba, A. H. (2023). A comprehensive review of biochar utilization for low-carbon flexible asphalt pavements. *Sustainability*, *15*(8). <https://doi.org/10.3390/su15086729>
- Yu, H., Bai, X., Qian, G., Wei, H., Gong, X., Jin, J., and Li, Z. (2019). Impact of ultraviolet radiation on the aging properties of SBS-modified asphalt binders. *Polymers*, *11*(7).  
<https://doi.org/10.3390/polym110711111>
- Yu, J. Y., Feng, P. C., Zhang, H. L., and Wu, S. P. (2009). Effect of organo-montmorillonite on aging properties of asphalt. *Construction and Building Materials*, *23*(7), 2636–2640.  
<https://doi.org/10.1016/j.conbuildmat.2009.01.007>
- Zakertabrizi, M., Hosseini, E., Sukumaran, S., Korayem, A. H., and Fini, E. H. (2021). Turning two waste streams into one solution for enhancing sustainability of the built environment. *Resources, Conservation and Recycling*, *174*.  
<https://doi.org/10.1016/j.resconrec.2021.105778>
- Zhang, X., Wang, J., Zhou, X., Zhang, Z., and Chen, X. (2021). Mechanical properties of the interfacial bond between asphalt-binder and aggregates under different aging conditions. *Materials*, *14*(5), 1–15. <https://doi.org/10.3390/ma14051221>
- Zhang, Y., Wang, Y., Kang, A., Wu, Z., Li, B., Zhang, C., and Wu, Z. (2022). Analysis of rejuvenating fiber asphalt mixtures' performance and economic aspects in high-

temperature moisture susceptibility. *Materials*, 15(21).  
<https://doi.org/10.3390/ma15217728>

Zhou, T., Xie, S., Kabir, S. F., Cao, L., and Fini, E. H. (2021). Effect of sulfur on bio-modified rubberized bitumen. *Construction and Building Materials*, 273.  
<https://doi.org/10.1016/j.conbuildmat.2020.122034>

## About the Authors

### **Mohammad Doroudgar**

Mohammad Doroudgar recently earned his master's degree in civil engineering from California State University, Long Beach (CSULB), specializing in transportation, pavement, and construction engineering. His research explores sustainable asphalt materials, focusing on low-carbon sulfur polymers, reclaimed asphalt pavement (RAP), and bio-based additives to improve durability and reduce environmental impacts. He has presented his work at national conferences and gained professional experience in construction management and infrastructure projects in Southern California.

### **Dr. Shadi Saadeh**

Dr. Shadi Saadeh joined the CSULB Civil Engineering and Construction Engineering Management Department in 2007. Dr. Saadeh worked for the Texas Transportation Institute (TTI) from 2003–2005 and the Louisiana Transportation Research Center (LTRC) from 2006–2007. He received his BSc in civil engineering from the University of Jordan (1997), MSc in Civil Engineering from Washington State University (2002), and PhD in Civil Engineering from Texas A&M University (2005).

Dr. Saadeh's research focuses on granular materials, including asphalt mixes and their constituents. His main areas of research are experimental characterization of highway materials, constitutive modeling of highway materials at the microstructural level, performance evaluation of highway infrastructure, flexible pavement design and analysis, and experimental characterization of highway materials using X-ray computed tomography (CT), image analysis techniques, and mechanical testing.

### **Dr. Elham Fini**

Dr. Ellie Fini is an Associate Professor at Arizona State University, an Invention Ambassador at the American Association for the Advancement of Science, a Fulbright Scholar of Aalborg University of Denmark, a Senior Sustainability Scientist at the Global Institute of Sustainability and Innovation, and Director of the Innovation Network for Materials, Methods and Management. Her research focuses on the design, synthesis, characterization, and atomistic modeling of novel materials to promote the sustainability and health of civil infrastructure.

In addition to more than 200 scholarly publications and numerous invited talks, her research has been featured by BBC Women in STEM, *Science Nation*, *Wired Magazine*, and CNBC. She is editor of the *ASCE Journal of Materials* and *Journal of Resources, Conservation and Recycling*. She has served as the president of ASCE's North Carolina Northern Branch and a program director of the

National Science Foundation. Her achievements have been recognized via multiple awards including an NSF CAREER award, ASEE Gerald Seeley award, BEYA Emerald STEM Innovation award, NC BioTech Research Excellence award, and WTS Innovative Transportation Solution award, to name a few.

# MTI FOUNDER

---

## Hon. Norman Y. Mineta

# MTI BOARD OF TRUSTEES

---

**Founder, Honorable Norman Mineta\*\*\***  
Secretary (ret.),  
US Department of Transportation

**Chair, Donna DeMartino**  
Retired Managing Director  
LOSSAN Rail Corridor Agency

**Vice Chair, Davey S. Kim**  
Senior Vice President & Principal,  
National Transportation Policy &  
Multimodal Strategy  
WSP

**Executive Director, Karen Philbrick, PhD\***  
Mineta Transportation Institute  
San José State University

**Rashidi Barnes**  
CEO  
Tri Delta Transit

**David Castagnetti**  
Partner  
Dentons Global Advisors

**Kristin Decas**  
CEO & Port Director  
Port of Hueneme

**Dina El-Tawansy\***  
Director  
California Department of  
Transportation (Caltrans)

**Anna Harvey**  
Deputy Project Director –  
Engineering  
Transbay Joint Powers Authority  
(TJPA)

**Kimberly Haynes-Slaughter**  
North America Transportation  
Leader,  
TYLin

**Ian Jefferies**  
President and CEO  
Association of American Railroads  
(AAR)

**Priya Kannan, PhD\***  
Dean  
Lucas College and  
Graduate School of Business  
San José State University

**Therese McMillan**  
Retired Executive Director  
Metropolitan Transportation  
Commission (MTC)

**Abbas Mohaddes**  
Chairman of the Board  
Umovity Policy and Multimodal

**Jeff Morales\*\***  
Managing Principal  
InfraStrategies, LLC

**Steve Morrissey**  
Vice President – Regulatory and  
Policy  
United Airlines

**Toks Omishakin\***  
Secretary  
California State Transportation  
Agency (CALSTA)

**Sachie Oshima, MD**  
Chair & CEO  
Allied Telesis

**April Rai**  
President & CEO  
COMTO

**Greg Regan\***  
President  
Transportation Trades Department,  
AFL-CIO

**Paul Skoutelas\***  
President & CEO  
American Public Transportation  
Association (APTA)

**Rodney Slater**  
Partner  
Squire Patton Boggs

**Lynda Tran**  
CEO  
Lincoln Room Strategies

**Matthew Tucker**  
Global Transit Market Sector  
Director  
HDR

**Jim Tymon\***  
Executive Director  
American Association of  
State Highway and Transportation  
Officials (AASHTO)

**K. Jane Williams**  
Senior Vice President & National  
Practice Consultant  
HNTB

\* = Ex-Officio  
\*\* = Past Chair, Board of Trustees  
\*\*\* = Deceased

---

## Directors

**Karen Philbrick, PhD**  
Executive Director

**Hilary Nixon, PhD**  
Deputy Executive Director

**Asha Weinstein Agrawal, PhD**  
Education Director  
National Transportation Finance Center Director

**Brian Michael Jenkins**  
Allied Telesis National Transportation Security Center

